NASA TN D-1066

TECHNICAL NOTE

D-1066

TRANSITION OF THE LAMINAR BOUNDARY LAYER ON A DELTA WING WITH 74° SWEEP IN FREE FLIGHT AT MACH NUMBERS FROM 2.8 TO 5.3

By Gary T. Chapman

Ames Research Center
Moffett Field, Calif.

NATIONAL AERONAUTICS AND SPACE ADMINISTRATION

WASHINGTON

August 1961

NATIONAL AERONAUTICS AND SPACE ADMINISTRATION

TECHNICAL NOTE D-1066

TRANSITION OF THE LAMINAR BOUNDARY LAYER ON A DELTA WING WITH 74° SWEEP IN FREE FLIGHT AT MACH NUMBERS FROM 2.8 TO 5.3

By Gary T. Chapman

SUMMARY

The tests were conducted at Mach numbers from 2.8 to 5.3, with model surface temperatures small compared to boundary-layer recovery temperature. The effects of Mach number, temperature ratio, unit Reynolds number, leading-edge diameter, and angle of attack were investigated in an exploratory fashion. The effect of heat-transfer condition (i.e., wall temperature to total temperature ratio) and Mach number can not be separated explicitly in free-flight tests. However, the data of the present report, as well as those of NACA TN 3473, were found to be more consistent when plotted versus temperature ratio. Decreasing temperature ratio increased the transition Reynolds number. The effect of unit Reynolds number was small as was the effect of leading-edge diameter within the range tested. At small values of angle of attack, transition moved forward on the windward surface and rearward on the leeward surface. This trend was reversed at high angles of attack (6° to 18°). Possible reasons for this are the reduction of crossflow on the windward side and the influence of the lifting vortices on the leeward surface.

When the transition results on the 74° delta wing were compared to data at similar test conditions for an unswept leading edge, the results bore out the results of earlier research at nearly zero heat transfer; namely, sweep causes a large reduction in the transition Reynolds number.

INTRODUCTION

Published information on boundary-layer transition at supersonic speeds on swept wings is limited. This problem was first studied briefly by Scott-Wilson and Capps (ref. 1). More detailed studies were made by Dunning and Ulmann (ref. 2). All of these studies were conducted in wind tunnels where the turbulence levels were probably high and the heat transfer essentially zero (adiabatic wall).

The purpose of the present report is to present transition results for a 74° swept delta wing in free flight and to compare these results with those of references 1 and 2 to see if heat transfer and free-stream turbulence affect the trends.

The present tests were conducted in the Ames Supersonic Free-Flight Wind Tunnel and Pressurized Ballistic Range facilities at Mach numbers from 2.8 to 5.3. Parameters whose effects were investigated included unit Reynolds number, temperature ratio, leading-edge diameter, and angle of attack. As is often the case when testing free-flight models, difficulties encountered in stabilizing and launching the test model at high speed placed a more severe limitation on the quantity of data obtained than had been originally anticipated. Nevertheless it was felt that the data were sufficient to indicate basic trends.

SYMBOLS

C_p pressure coefficient, $\frac{p - p_\infty}{(1/2)\rho U^2}$

D diameter of leading edge, in.

h maximum peak-to-valley height of roughness scratches, in.

M Mach number

p local static pressure

R Reynolds number based on x, $\frac{\rho U x}{\mu}$

R_T transition Reynolds number, based on length of laminar flow, $\frac{\rho U x_l}{\mu}$

T temperature

U total velocity, ft/sec

x distance from leading edge parallel to center line, in.

α angle of attack, deg

φ angle of roll, deg

Λ sweep angle of wing leading edge, deg

μ coefficient of viscosity, slugs/ft sec

ρ density, slugs/ft^3

Subscripts

l laminar

w wall conditions

o free-stream stagnation conditions

∞ free-stream static conditions

MODEL AND TEST CONDITIONS

The models described in this report were launched from a 57-mm smooth-bore gun. The tests conducted at Mach numbers 2.8 to 4.1 were in still air in two facilities, the Ames Supersonic Free-Flight Wind Tunnel (ref. 3) and the Pressurized Ballistic Range.

The Pressurized Ballistic Range is essentially a pressure vessel 10 feet in diameter and 200 feet long. It is internally instrumented to take sets of orthogonal shadowgraph pictures at various intervals along the flight path. For present purposes, it has two important advantages over the supersonic free-flight wind tunnel. First, the pressure level can be adjusted so as to vary the unit Reynolds number; and second, the optics are free of any mirrors, lenses, or windows which tend to impair the quality of the shadowgraphs.

The models tested at Mach number 5.3 were fired upstream through the supersonic free-flight wind tunnel operating at a Mach number of 2 (i.e., air on). Here again, each of the models with its flow field was observed in flight by means of a set of orthogonal shadowgraph pictures taken at intervals along the flight path. A description of the wind tunnel and some of the associated equipment may be found in reference 3. Table I lists the models with their associated test conditions.

Model Geometry

The models tested were 74° swept delta wings of biconvex cross section (fig. 1). The surface of wing contour was generated by turning the model as a section of a cone (see insert in fig. 1). The model was constructed of two metals - phosphor bronze and magnesium. The use of the two metals was required to obtain an adequate static stability margin.

Figure 2 shows a model with the sabot used in most of the tests. Other types of sabots were also tried but were less successful. The sabot is a split-cup type, in which the model is held by a screw which

is on the parting line of the sabot. The sabot is made of nylon with an aluminum mounting plate to distribute the launching load of the model.

Model Surface and Leading-Edge Geometry

It is well known that surface roughness and leading-edge size and shape can affect boundary-layer transition. For this reason these variables were closely controlled.

Surface finish.- All of the models tested were polished with fine emery paper, using the method described in reference 4. The final surface was examined under a microscope to make sure the surface was uniform. Figure 3(a) shows some typical photomicrographs taken of the surfaces. In general, the scratches were parallel to the generators of the conical surface.

The surface roughness was held constant for most of the tests. The maximum value of roughness height, h, was 50 microinches. This gave a maximum roughness parameter $(h/\delta)\sqrt{Re}$ of 15 for a nominal Reynolds number, 8 million, based on length of model, at Mach number 3.3. This is well below the critical value for two-dimensional roughness for that Mach number given in reference 5. Smoother surfaces were not used because of the expense and time required to achieve them.

Leading edge.- The leading edges were initially square with a forward face of uniform width. The width of this flat face was chosen as the diameter of the finished leading edge. The edge was then hand-finished with fine emery paper to a semicircular shape. The leading-edge diameter was varied from 0.0006 inch to 0.006 inch for the Mach number 3.3 tests and was held between 0.012 and 0.016 inch for the Mach number 5.3 tests. Figure 3(b) shows two views of the leading edge for the same model.

In the region of the apex the plan form of the model tended to round off as a result of polishing. The apex, however, was kept as symmetrical as possible, in both planes. Figure 3(c) shows two sets of plan-form and profile views, corresponding to two different leading-edge diameters.

Test Conditions

Mach number and Reynolds number.- Tests were made at Mach numbers between 2.8 and 4.1, and at 5.3, with wind-tunnel flow Mach numbers of 0 and 2, respectively. A nominal unit Reynolds number of 2 million per inch was used throughout most tests; however, for one series of tests the unit Reynolds number was varied from 0.4 to 2 million per inch.

Surface temperature.- The models tested were at ambient temperature prior to launch. The surface temperature was assumed to remain unchanged throughout the flight, which was of a very short duration (7 to 14 milliseconds). The justification for this assumption may be found in references 5 and 6. The ratios of wall temperature to free-stream total temperature were 0.32 and 0.27 for Mach numbers of 3.3 and 5.3, respectively.

Pressure distribution.- Because of the finite thickness and shape of the model, a sizable streamwise pressure gradient existed. The pressure gradient was not determined experimentally, but was estimated to be approximately twice as large as for a wing comparable in plan form and profile at a fixed streamwise location, but with a diamond-shaped cross section normal to the plane of symmetry. In figure 4 a pressure distribution is presented for a fixed spanwise location on the model of the present tests and for the comparison wing mentioned above. This estimate was based on linearized theory for sharp leading-edged swept wings.

Determination of the Point of Transition

Ideally, three different criteria for locating transition were applied to each set of shadowgraphs in order to define the transition boundary. In order to illustrate these criteria, an isometric drawing of the model and the associated set of orthogonal shadowgraphs is shown in figure 5. The model is depicted in the drawing as rolled φ degrees with respect to the light reference axis. The dotted lines on the model surface represent the transition boundary. Also shown is the top element of the conical surface which is observed in the side projection.

Transition on model center line.- The first criterion for determining the point of transition is the appearance of wavelets in the flow field near the boundary layer. These wavelets are associated with spots of turbulence. The forward end of the envelope enclosing these wavelets is assumed to be the most forward point of transition and is assumed to lie on the model center line. This point is located in the profile view of figure 5 by arrow A. Cases where the center-line ray was observed in profile (i.e., no roll) showed this to be a good assumption. Due to the small amount of curvature of the model surface this point could be located through a roll angle range of $\pm 15^{\circ}$. Figure 6(a) shows a profile shadowgraph of a model in flight. The arrows marked A indicate typical examples of transition points located according to this first criterion.

Transition on a ray.- The second criterion for determining the transition point is the first occurrence of disturbances in the diffraction lines along the edges of bodies having laminar boundary layers. The model surface, being conical, permitted the observance of individual rays, with the particular ray depending on the roll attitude. In figure 5 the intersection of the ray observed in the profile view and the transition boundary is marked with a cross on the model surface and is indicated

by arrow B in the profile view. This point occurs downstream of the transition point on the plane of symmetry, consistent with observations made by other flow visualization techniques, such as china clay or luminous lacquers (ref. 2). In figure 6(b) points located by the above method are marked with arrows B.

Transition point on trailing edge from wake study.- From studies of the wake in plan-form-view shadowgraphs the line of division between laminar and turbulent sheets coming off the wing could be determined. The intersection of this line with the model trailing edge locates a point on the transition boundary. Again referring to figure 5, the arrows marked C in the plan-form view indicate the transition boundary at the trailing edge. Figures 6(c) and 6(d) show typical plan-form shadowgraphs. The points on the transition boundary found by this method are marked by arrows. It was found that the points determined by this method were consistent with the results obtained by observations along a ray. This method of determining the point of transition really defines a value for either the upper or lower surface, on whichever surface transition occurs first, and is useful only at small angles of attack. This method could not be used for air-on tests because the turbulent boundary layer on the tunnel windows obliterated the laminar wake of the model.

Accuracy of Results

To check the reading accuracy of the transition-point measurements, all data points were read at least twice. In a few cases the point of transition was read by two different individuals. For the first two methods of measuring transition (i.e., on center line and on ray) the results, as read by the two different individuals, agreed in most cases within 0.20 inch. When deviations between two readings became larger than 0.20 inch, the data point was re-evaluated or left out. The measurements of transition at the trailing edge were not as accurate as the others because small changes in the spanwise location of the intersection of the transition boundary and the trailing edge resulted in larger errors in the length of laminar run. However, this uncertainty was less than 0.30 inch.

The presence of the joint in the model surface caused some question as to its effect on transition occurring near or downstream of it. In figure 6 weak shock waves can be seen emanating from the joint. It was concluded, however, on the basis of the data which will be shown in the next section, that this effect was generally small (i.e., within the randomness of transition).

The accuracy of measurement of other pertinent quantities is as follows:

Mach number, M_∞	± 0.05
Unit Reynolds number, R_∞/x	$\pm 0.05 \times 10^6$ per in.
Angle of attack, α	$\pm 0.20^\circ$
Roll angle, φ	$\pm 0.5^\circ$

RESULTS AND DISCUSSION

Transition Pattern

Figure 7 shows the transition patterns on the plan form of all the test models except those which experienced fully laminar flow. The circles represent data points obtained from the profile-view shadowgraphs by the first two methods described in this report (i.e., transition on plane of symmetry and transition on observed ray). The squares represent data points obtained from plan-form-view shadowgraphs by the study of the wake. When the angle of attack was significantly different from zero, as was the case in all but figure 7(a), the leeward and windward transition points were represented by open and solid circles, respectively. In a few cases there was no evidence of transition on the observed ray (i.e., transition behind trailing edge). These points are indicated with arrows pointing downstream of the trailing edge. Also shown in figure 7 are the actual and theoretical apexes for each test model and the location of the bimetallic joint. Included for reference are two dotted lines parallel to the leading edge. These lines are 1 and 2 inches, respectively, from the leading edge, measured parallel to the free stream.

In figure 7, it should be noted that the transition points downstream of the bimetallic joint generally lie about a line parallel to the leading edge which passes through the transition points ahead of the bimetallic joint (i.e., the transition front is parallel to the leading edge). This is what Dunning and Ulmann (ref. 2) found from tests on swept flat plates and on swept wings with NACA 65A004 airfoils. The transition front parallel to the leading edges is apparently typical of both subsonic and supersonic flow over swept wings. From this, it appears that the effect of the bimetallic joint on transition was small except on model 5 which was subjected to the greatest launch stress.

Effect of Mach Number and Temperature Ratio

For tests conducted in free flight, the Mach number and temperature ratio are not independent (i.e., increasing flight velocity decreases the temperature ratio). Therefore, the transition results are plotted

versus both Mach number and temperature ratio, as shown in figure 8. In figure 8 the range of transition Reynolds number, due to randomness of transition and angle of attack, is given by the bars. The symbols represent a transition Reynolds number based on the distance (parallel to the free stream) to a line parallel to the leading edge about which the transition boundary fluctuates. In figure 8(a) the transition results are plotted versus Mach number. When plotted in this manner, there appears to be an increase in transition Reynolds number with increasing Mach number, at Mach numbers from 2.9 to 4.1. However, the results for Mach number 5.3, which were obtained with air flow counter to the direction of model flight (i.e., air-on testing), are contrary to this trend. Two possible reasons for this change are that the temperature ratio has increased and the turbulence level has increased, both of which resulted from the air-on testing.

For comparison, the unpublished results for a 75° swept flat plate and for a 72° swept flat plate (ref. 2) are shown. The unpublished data were obtained by Jillie and Hopkins in a small blowdown facility at the Ames Research Center. The general trend of the results of the present tests, between Mach numbers 2.9 and 4.1, agrees with the trend exhibited by the other results. There is, however, a large difference in the absolute level of the results. The free-flight tests give transition Reynolds numbers which are four to six times greater than the wind-tunnel results. There are two reasons which could possibly account for this difference in level of the data: first, the free-flight tests were for relatively high heat transfer to the model, whereas the wind-tunnel tests were for an adiabatic wall (i.e., zero heat transfer); and second, in the free-flight tests the free-stream turbulence was small, whereas the free-stream turbulence for the unpublished wind-tunnel tests was quite high. Both of these conditions are known to influence transition.

When the data of figure 8(a) are replotted as a function of temperature ratio (i.e., heat-transfer condition) as in figure 8(b), two interesting facts appear. It is seen that the data indicate a uniform trend of decreasing transition Reynolds number with increasing temperature ratio. The agreement of the data for Mach number 5.3 (triangular symbols) with the other data may be fortuitous because the effects of Mach number and turbulence level would be in the opposite directions. For comparison, again the wind-tunnel results are presented. It is seen that these data agree fairly well with the trend established by the present data. From figure 8(b) it seems plausible that the heat-transfer condition rather than free-stream turbulence accounts for most of the difference in level of the transition Reynolds number observed in figure 8(a).

Effect of Unit Reynolds Number

The effect of unit Reynolds number on transition Reynolds number is shown in figure 9. At low values of unit Reynolds number, transition occurred in the wake of model. These points are indicated, in figure 9, by Reynolds numbers based on the maximum length of model, with arrows pointing toward possible higher values. The results at a unit Reynolds number of 0.75 million per inch (model number 31) were for high angle of attack. The bar indicates the lowest value for angles less than 6°. The maximum value of transition Reynolds number, for angles less than 6°, is indicated by an arrow (i.e., transition occurred in wake). The triangular symbol denotes the approximate zero angle-of-attack value. The data at higher unit Reynolds numbers are denoted by bars to indicate maximum and minimum values, and symbols to denote averages. Because of the wide variation in transition Reynolds number due to randomness and angle-of-attack variation, and the inconclusive results at low values of unit Reynolds number, no definite conclusion could be drawn from the data alone. However, when the results are compared against the free-flight results for a 25° cone-cylinder (ref. 7) for the same conditions, it can be seen that the effect of unit Reynolds number in the present results must be considerably less than in the results of reference 7 or transition would have occurred on the wing at the low values of unit Reynolds number instead of in the wake.

Effect of Leading-Edge Diameter

Figure 10 shows that increasing the leading-edge diameter has no detectable effect on transition Reynolds number, at least in the range tested. Here again the variation of the results is indicated by bars, with symbols indicating averages. For comparison, the transition results for a 60° swept flat plate (ref. 2) are shown. Here again there is no appreciable effect of changing the leading-edge diameter.

Effect of Angle of Attack

It was possible to obtain data on the effect of angle of attack on transition in the low angle-of-attack range for high Reynolds number (order of 9 million). It was further possible to define the effect of large angles of attack on transition for low values of Reynolds numbers (order of 3 million). These results are discussed in the following paragraphs.

Low angles of attack.- Figure 11(a) shows the effect of small angles of attack on transition Reynolds number. When the angle of attack was small, the randomness of transition tended to overshadow small changes

due to angle of attack. Two runs, at Mach numbers of 4.1 and 5.3, had sufficient angle of attack to be measured with accuracy. The data at Mach number 3.3 (not shown in this figure) had angles less than 0.50°. The data for Mach number 4.1 (data represented by circles) show some increase of laminar flow on the leeward side, as compared to the windward side. This is not the case for the Mach number 5.3 data (represented by squares) where no detectable change is evident within the scatter caused by randomness of transition and reading error. Two variables were different between the two sets of data, which may explain this apparent disagreement. At Mach number 4.1 the component of Mach number normal to the leading edge was slightly subsonic, and at 5.35 the normal Mach number was supersonic; also the leading edges were 0.0015 and 0.012-0.016 inches in diameter, respectively. There was not sufficient information available to determine which, if either, of these was the cause of the change.

For comparison, the results of reference 2 for a 60° swept flat plate at Mach number 4.04 are shown (dashed line). This trend is the same as that shown by the Mach number 4.1 data. The reason for this trend is probably associated with the change in local Reynolds number due to expansion and compression of the flow (ref. 2). However, because of the complex nature of the flow over the wing, no attempt was made to correlate the data on this basis.

High angles of attack.- The results for large angles of attack are presented in figure 11(b). The data are for a Mach number of 2.9 and a unit Reynolds number of 0.75 million per inch. It can be seen that the trend on the leeward side has now reversed, and the length of laminar run is now decreasing with angle of attack. This reversal seems to be caused by the presence of the strong lifting vortices which are turbulent and are shedding strong acoustical radiation onto the boundary layer. Figure 12 shows two wings at large angles of attack. The strong lifting vortices, passing close to the leeward surface of the wing, are plainly evident in each case. The transition Reynolds number of the wing in figure 12(a) was plotted versus angle of attack in figure 11(b).

No definite trend could be established on the windward side at large angles of attack, because transition occurred off the wing. The transition Reynolds number, based on center-line chord, was greater than 2.75 million at angles of attack greater than 6°. This is about that obtained at zero angle of attack at high unit Reynolds number. The apparent increase of laminar flow on the windward side may be associated with a change in the controlling boundary-layer instability mechanism (ref. 7) resulting from a reduction in the crossflow velocity component at large angles of attack on the windward surface. This reduction in crossflow is more easily understood if one realizes that the direction of crossflow at zero angle of attack is inboard. As the wing goes to angle of attack, the pressure near the model plane of symmetry becomes higher, reducing the flow velocity toward the center line and, at sufficiently high angles of attack, there is an outward crossflow.

Wake Observations

Figure 13 shows shadowgraphs of the model wake in plan form. These shadowgraphs show a system of vortices, in the wake immediately downstream of the trailing edge, of the type first observed by Owen and Randall (ref. 8) at subsonic speeds and later by Scott-Wilson and Capps at Mach number 1.61 (ref. 1). They have also been observed at Mach number 6 by Seiff and Wilkins (ref. 9). A similar-type phenomenon has been observed by Fujii (ref. 10) in the free convection boundary layer along a vertical flat plate. The similarity arises from the similarity in shape of the free convection boundary-layer velocity profile to the crossflow boundary-layer velocity profile on a swept wing. This velocity profile has an inflection point which is thought to be the cause of the vortex formation.

The spacing of these vortices was measured and found to vary from 0.075 inch at the center line to 0.040 inch near the wing tips. These measurements were taken from plan-form-view shadowgraphs of the model in flight at a free-stream Mach number of 3.48 and a unit Reynolds number of 0.38 million per inch. The boundary layer was laminar coming off the base. The patches of turbulence observed in figures 13(a) and (b) are the lifting vortices trailing back over the model. One of the wing tips of the model was damaged on launch, but it does not affect the flow over the wing, except behind the Mach line from the initial disturbance, or some small distance ahead of the Mach line due to pressures felt through the subsonic portion of the boundary layer.

Effect of Sweep on Transition

Although sweep was not a variable of the present set of tests, the over-all effect of sweep could be inferred by comparing the result of the swept wing of the present test to other free-flight data for similar free-stream conditions but with unswept leading edges. Figure 14 shows such a comparison for two data points of the present test at Mach numbers of 3.3 and 5.3 (open diamond and triangle) which have been normalized by dividing by transition Reynolds numbers at zero sweep from reference 5. The results of reference 5 were obtained from tests of transition location on the outer surfaces of sharp leading edge (D = 0.00025 inch) hollow tubes.

Data on the effect of sweep at zero heat transfer (ref. 2) are also presented in this figure. The normalizing value of transition Reynolds number used for the flat plate, from reference 2, was for an unswept plate with the same leading-edge thickness (D = 0.002 to 0.003 inch).

It can be seen that the results of the present test are substantially in agreement with the results of reference 2 in showing an extreme

reduction in transition Reynolds number with increasing sweep. This is true even though there was a large difference in heat-transfer condition between the present tests and reference 2. It should be pointed out that the leading edges of the present test model was considerably blunter than the leading edge of the model from which the normalizing value was obtained. Since slight blunting of unswept leading edges increases lengths of laminar flow (ref. 11), the free-flight results shown in figure 14 would probably be somewhat lower if normalized by results for an unswept wing with an equal amount of bluntness. This would put the results somewhat below those of reference 2 which would not be surprising because the wing of the present test has a sizable spanwise pressure gradient which is known to have an adverse effect on transition (ref. 8).

SUMMARY OF RESULTS

Results have been presented for transition on a delta wing with 74° of sweep. The tests were made in free flight at supersonic speeds, under cold-wall conditions. These results were compared to results of wind-tunnel tests on swept wings. Following is a summary of some of the results.

The reduction in transition Reynolds number due to sweep, noted subsonically and in wind-tunnel tests at supersonic speeds, is corroborated by these free-flight tests at Mach numbers from 2.8 to 5.3. The transition front was found to be essentially parallel to the leading edge. When transition occurred in the wake, a system of streamwise vortices was detected in the wake upstream of the point of transition. The transition Reynolds number was found to increase with increasing Mach number and increasing heat transfer to the model (i.e., decreasing wall temperature to stagnation temperature ratio) and to correlate on the basis of temperature ratio with results of wind-tunnel tests at nearly zero heat transfer. In the range tested, transition was found to be relatively unaffected by leading-edge diameter. At high angles of attack, transition moved forward on the leeward surface under the adverse influence of the lifting vortices. On the windward surface, transition moved rearward as the result of a reduction in crossflow.

Ames Research Center
National Aeronautics and Space Administration
Moffett Field, Calif., May 9, 1961

REFERENCES

1. Scott-Wilson, J. B., and Capps, D. S.: Wind Tunnel Observations of Boundary Layer Transition on Two Sweptback Wings at a Mach Number of 1.61. RAE Tech. Note Aero 2347, Dec. 1954.

2. Dunning, Robert W., and Ulmann, Edward F.: Effect of Sweep and Angle of Attack on Boundary-Layer Transition on Wings at Mach Number 4.04. NACA TN 3473, 1955.

3. Seiff, Alvin: A Free-Flight Wind Tunnel for Aerodynamic Testing at Hypersonic Speeds. NACA Rep. 1222, 1955.

4. Wilkins, Max E., and Darsow, John F.: Finishing and Inspection of Model Surfaces for Boundary-Layer-Transition Tests. NASA MEMO 1-19-59A, 1959.

5. James, Carlton S.: Boundary-Layer Transition on Hollow Cylinders in Supersonic Flight as Affected by Mach Number and a Screwthread Type of Surface Roughness. NASA MEMO 1-20-59A, 1959.

6. Jedlicka, James R., Wilkins, Max E., and Seiff, Alvin: Experimental Determination of Boundary-Layer Transition on a Body of Revolution at $M = 3.5$. NACA TN 3342, 1954.

7. Potter, J. L.: New Experimental Investigations of Friction Drag and Boundary Layer Transition on Bodies of Revolution of Supersonic Speeds. NAVORD Rep. 2371, April 1952.

8. Owen, P. R., and Randall, D. G.: Boundary Layer Transition on a Sweptback Wing. RAE Tech. Memo. Aero. 277, May 1952.

9. Seiff, Alvin, and Wilkins, Max E.: Experimental Investigation of a Hypersonic Glider Configuration at a Mach Number of 6 and Full-Scale Reynolds Numbers. NASA TN D-341, 1961.

10. Fujii, Tetsu: On the Development of a Vortex Street in a Free Convection Boundary Layer. Bulletin of Japan Society of Mechanical Engineers, vol. 2, no. 8, Nov. 1959, pp. 551-555.

11. Brinich, Paul F.: Effect of Leading-Edge Geometry on Boundary-Layer Transition at Mach 3.1. NACA TN 3659, 1956.

TABLE I.- TEST CONDITIONS FOR VARIOUS MODELS

Model no.	M_∞	D	$h \times 10^6$	$\frac{R_\infty}{x} \times 10^{-3}$, per in.	T_w/T_o	Remarks
5	4.1	0.0015	30	2.86	0.23	air off
15	3.35	.006	50	1.90	.31	
17	3.24	.0006	50	1.84	.32	
21	2.81	.006	50	1.66	.39	
24	5.33	.012	30	2.18	.27	air on
25	5.31	.016	30	2.06	.27	
28	3.27	.015	30	.525	.32	air off
29	3.48	.020	30	.378	.29	
30	3.02	.003	10/50	1.70	.351	
31	2.90	.012	50	.74	.371	

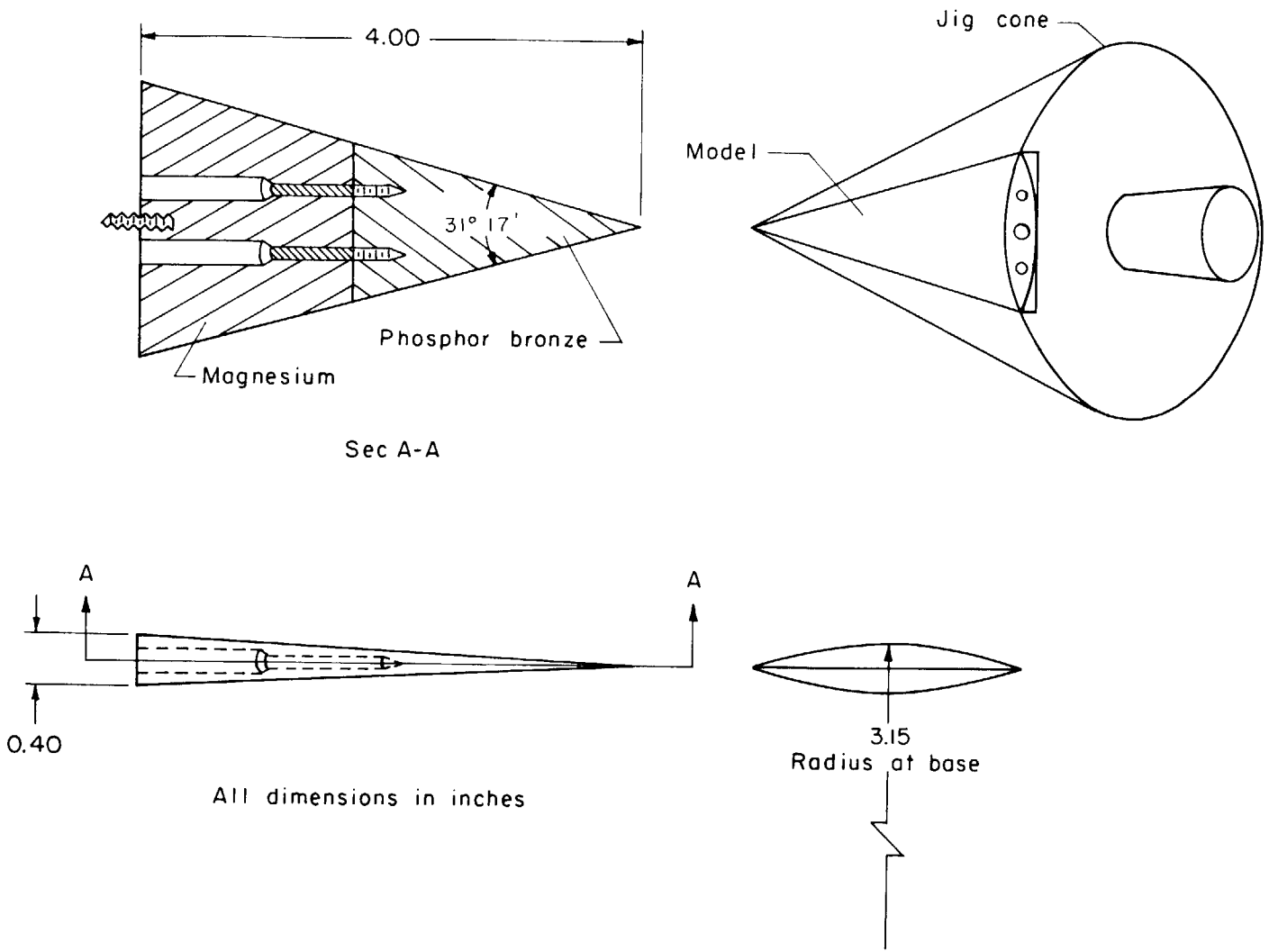

Figure 1.- Delta-wing model.

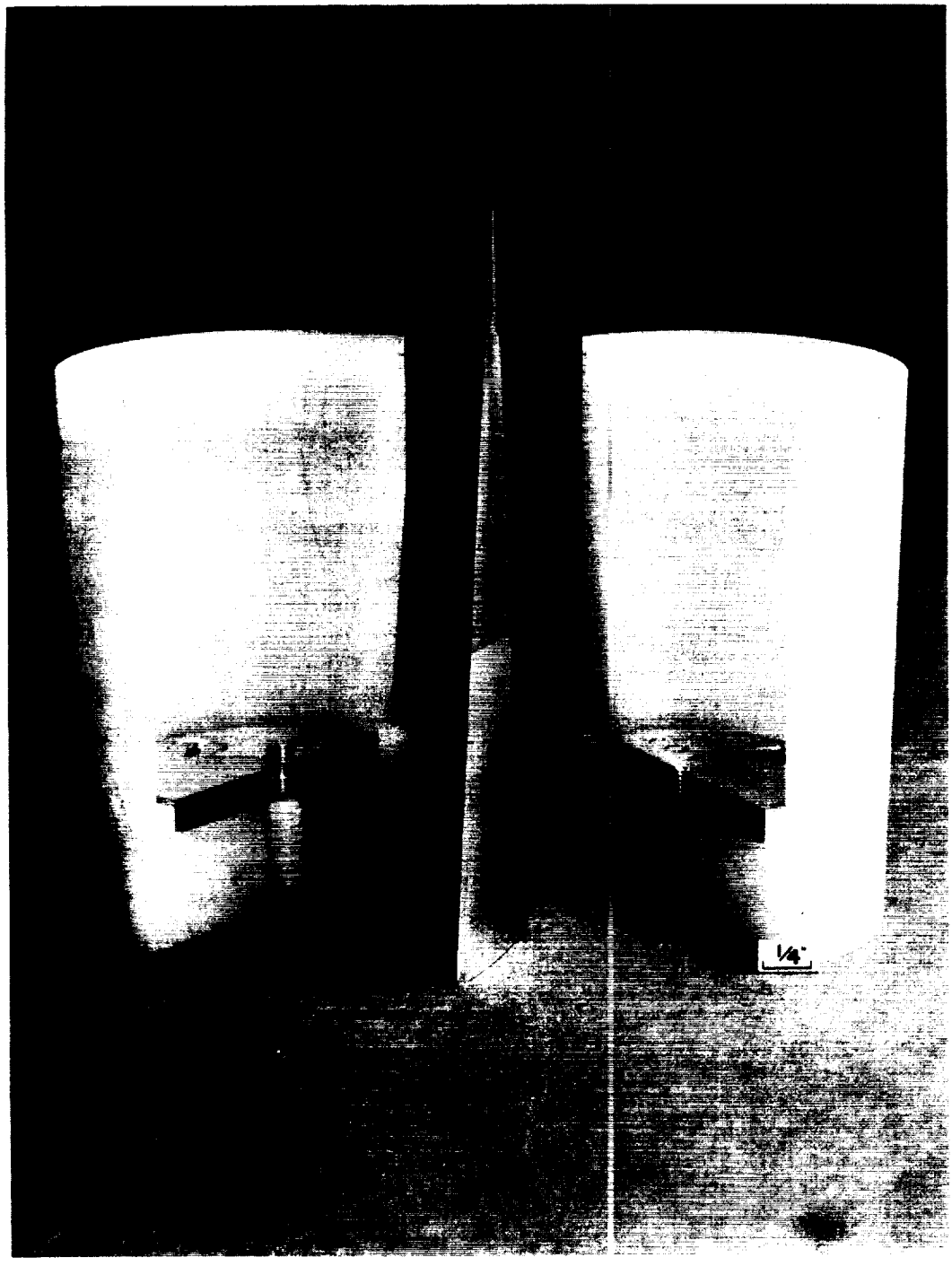

A-27089

Figure 2.- Delta-wing model and sabot.

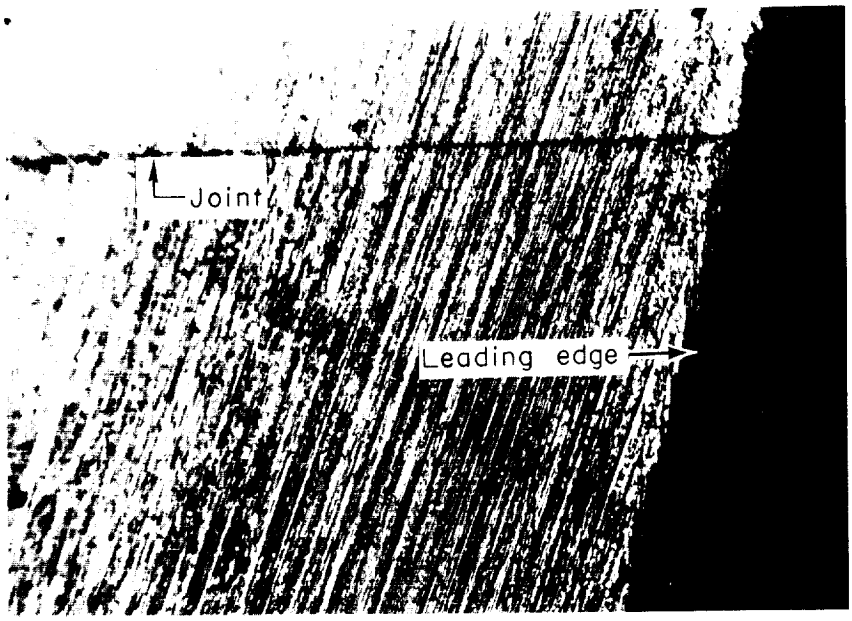

Model 13, h_{max} = 50 microinches.

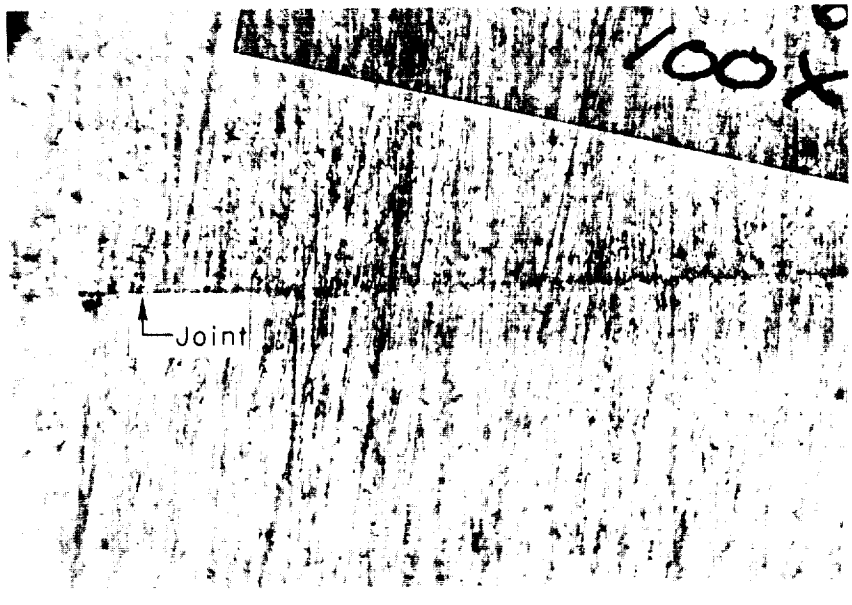

Model 21, h_{max} = 50 microinches.

(a) Surface finish.

Figure 3.- Photomicrographs of the model, 100X.

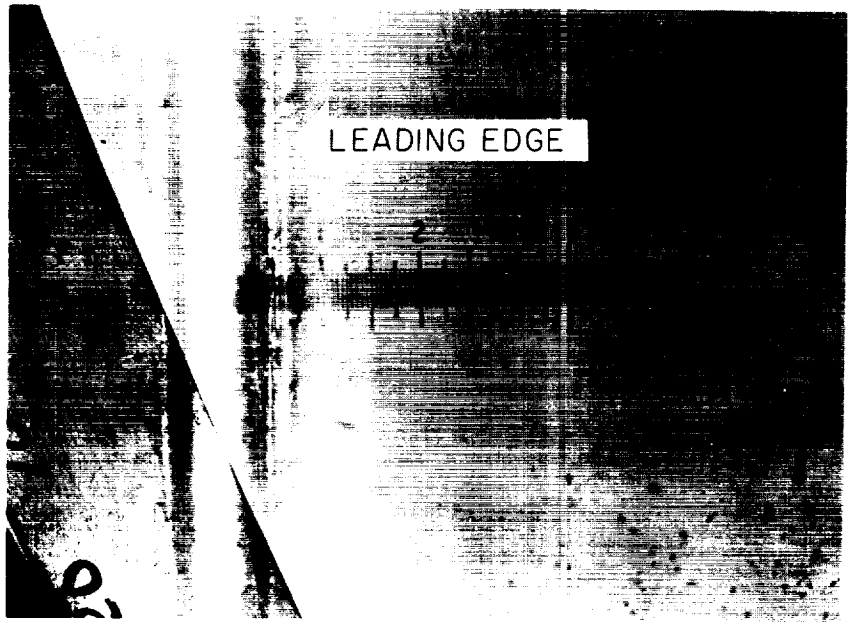

Edge-on view.

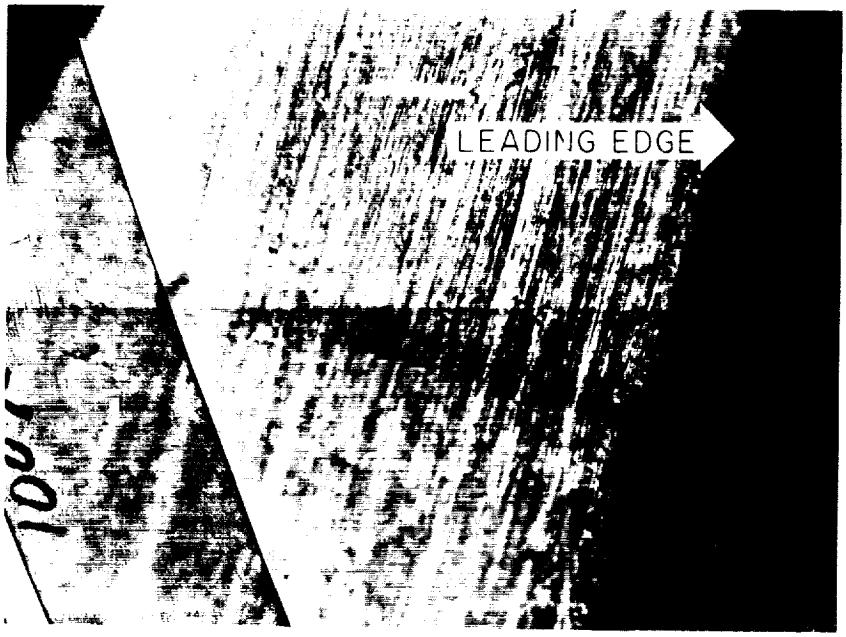

Plan-form view. A-27111.1

(b) Leading-edge views of model 20; D = 0.005 in.

Figure 3.- Continued.

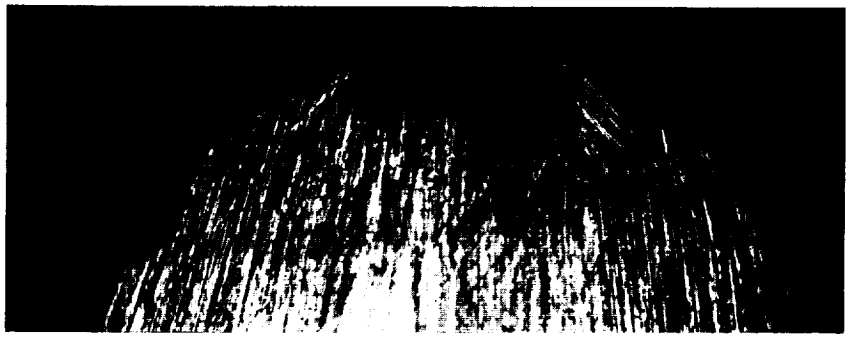

Model 17, D = 0.0006 in., plan-form radius 0.025 in.

Model 21, D = 0.006 in., plan-form radius 0.045 in.

Plan-form views.

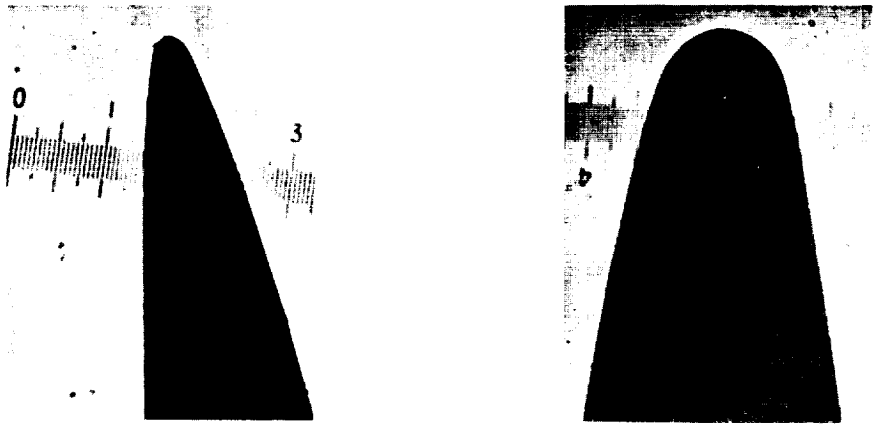

Model 17, D = 0.0006 in., profile radius 0.002 in.

Model 21, D = 0.006 in., profile radius 0.003 in.

Profile views.

(c) Model apex.

Figure 3.- Concluded.

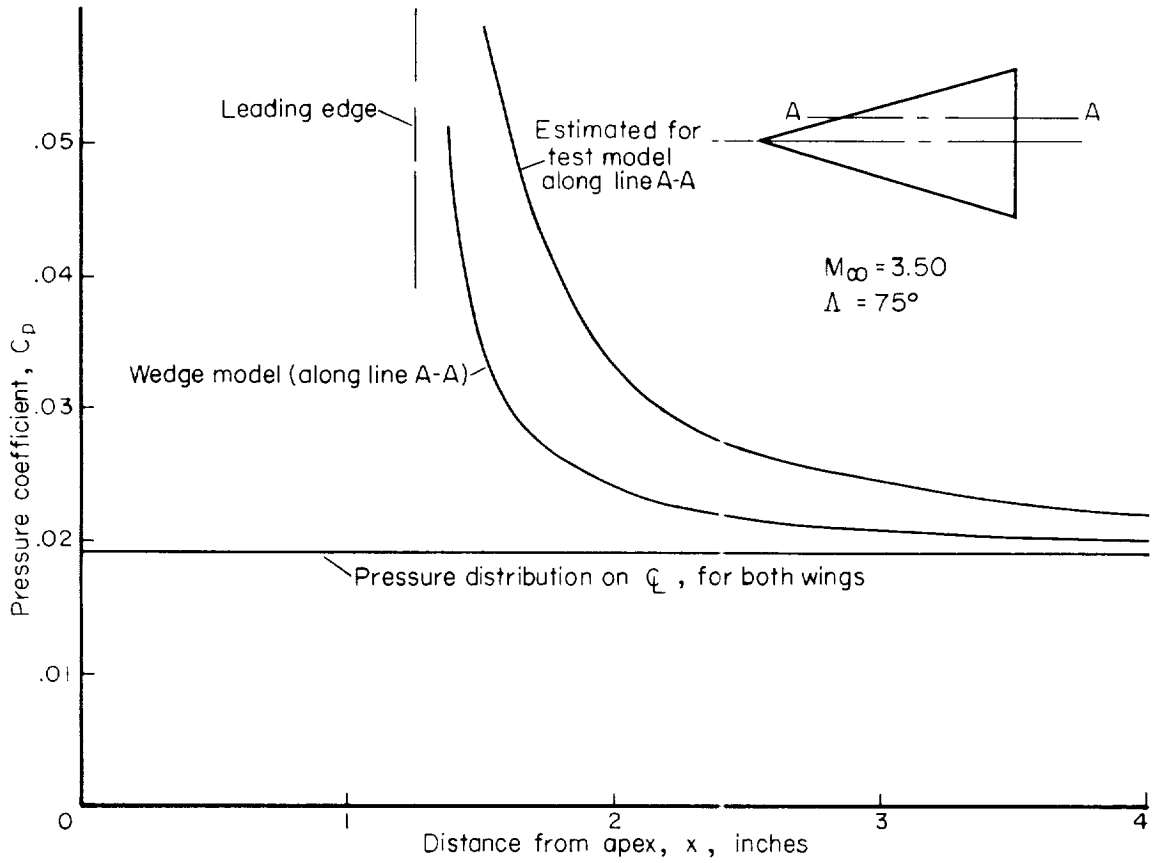

Figure 4.- Typical pressure distribution.

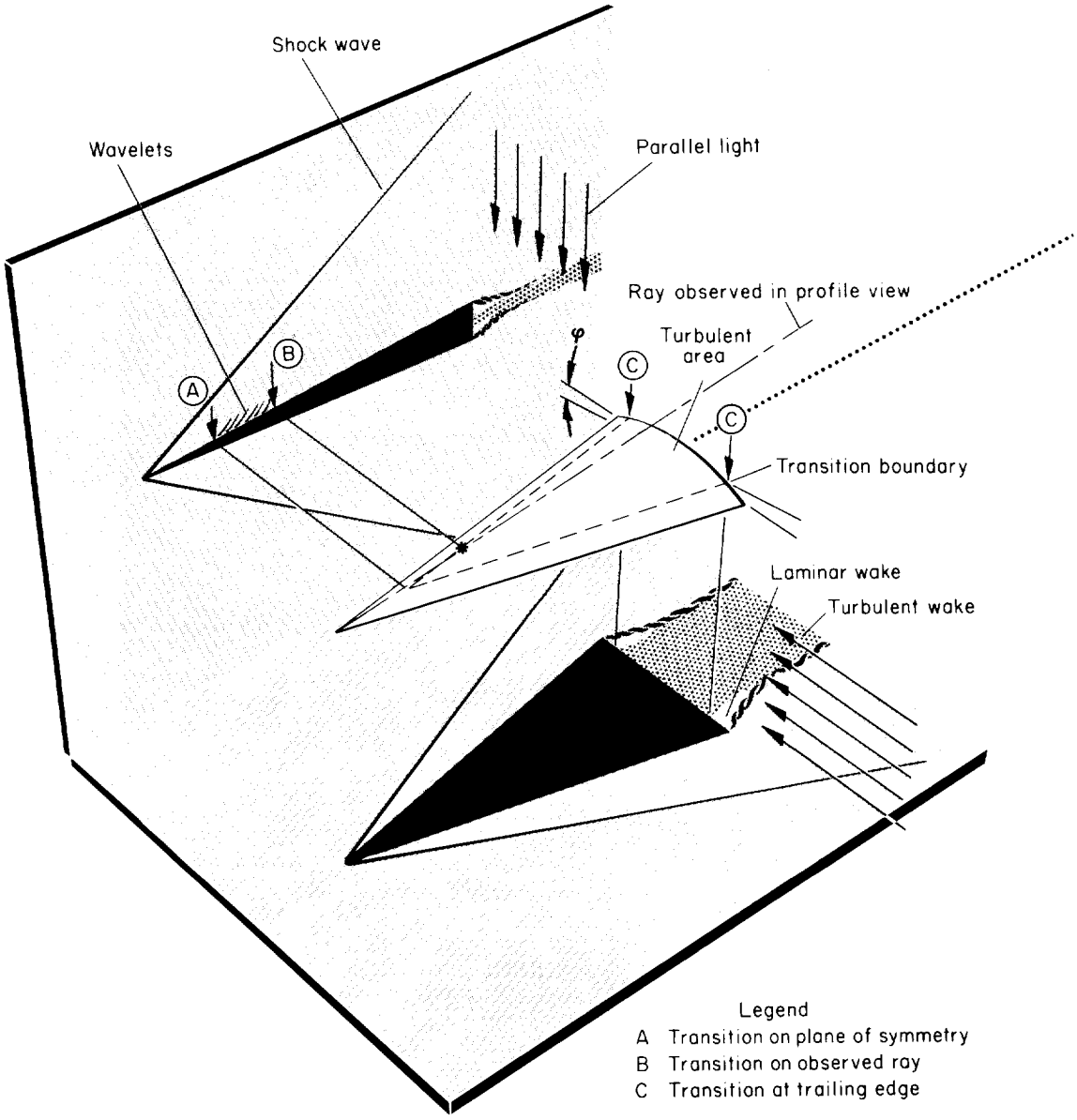

Figure 5.- Isometric drawing of model and associated shadowgraphs.

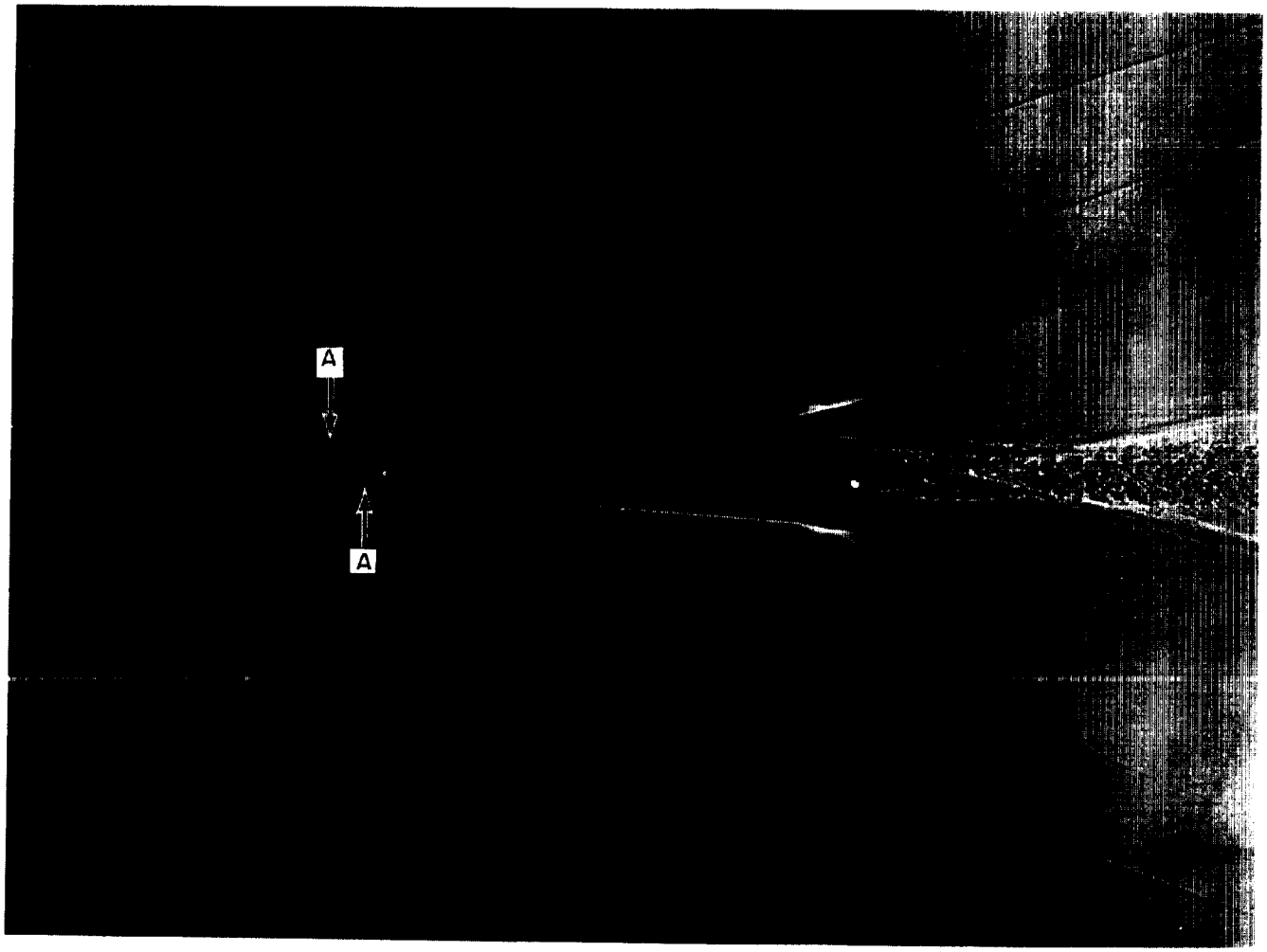

A-27070-A.1

(a) Profile view of model 17; $M_\infty = 3.24$.

Figure 6.- Typical shadowgraphs of model in flight.

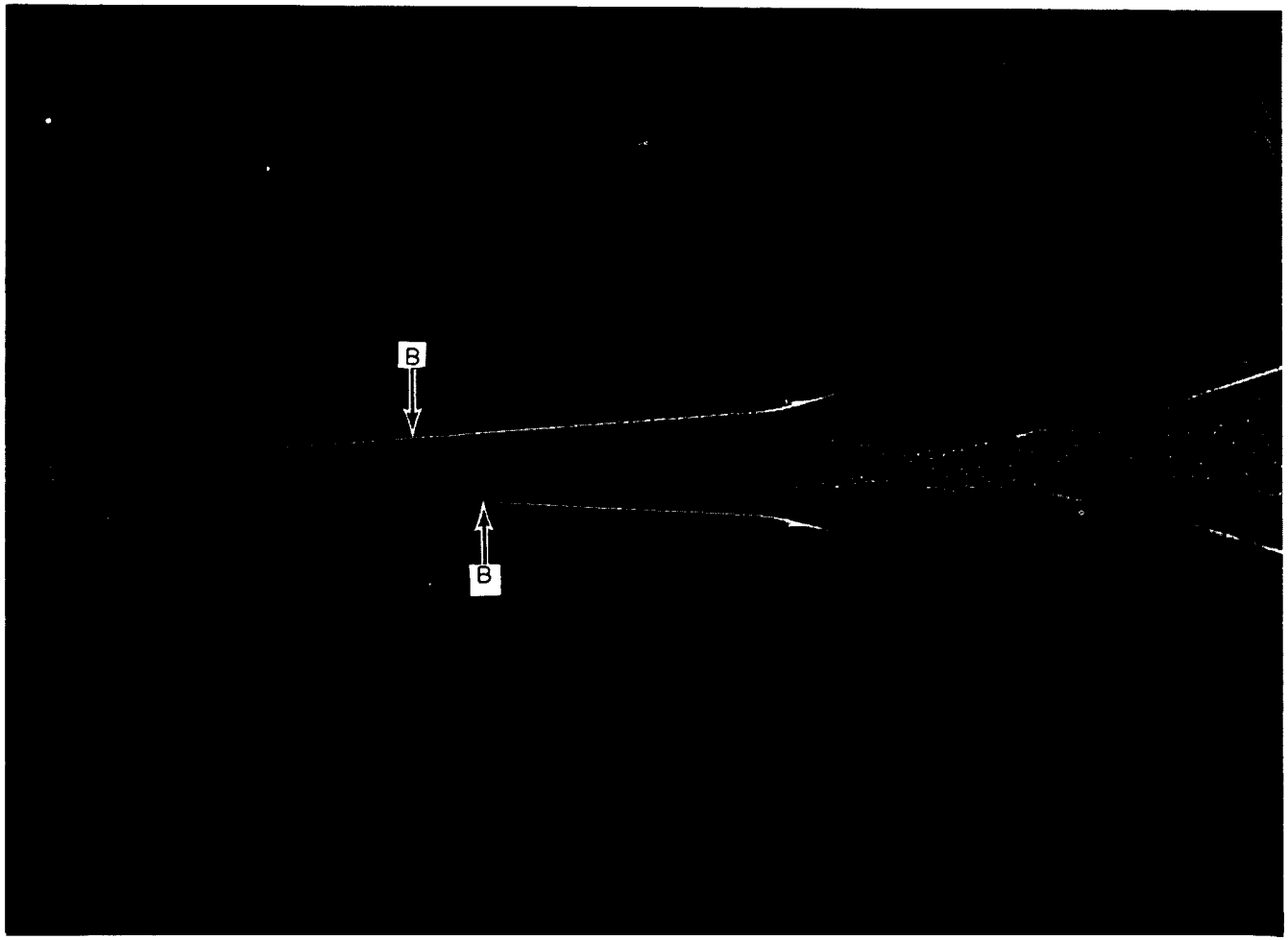

A-27070-B.1

(b) Profile view of model 21; $M_\infty = 2.81$.

Figure 6.- Continued.

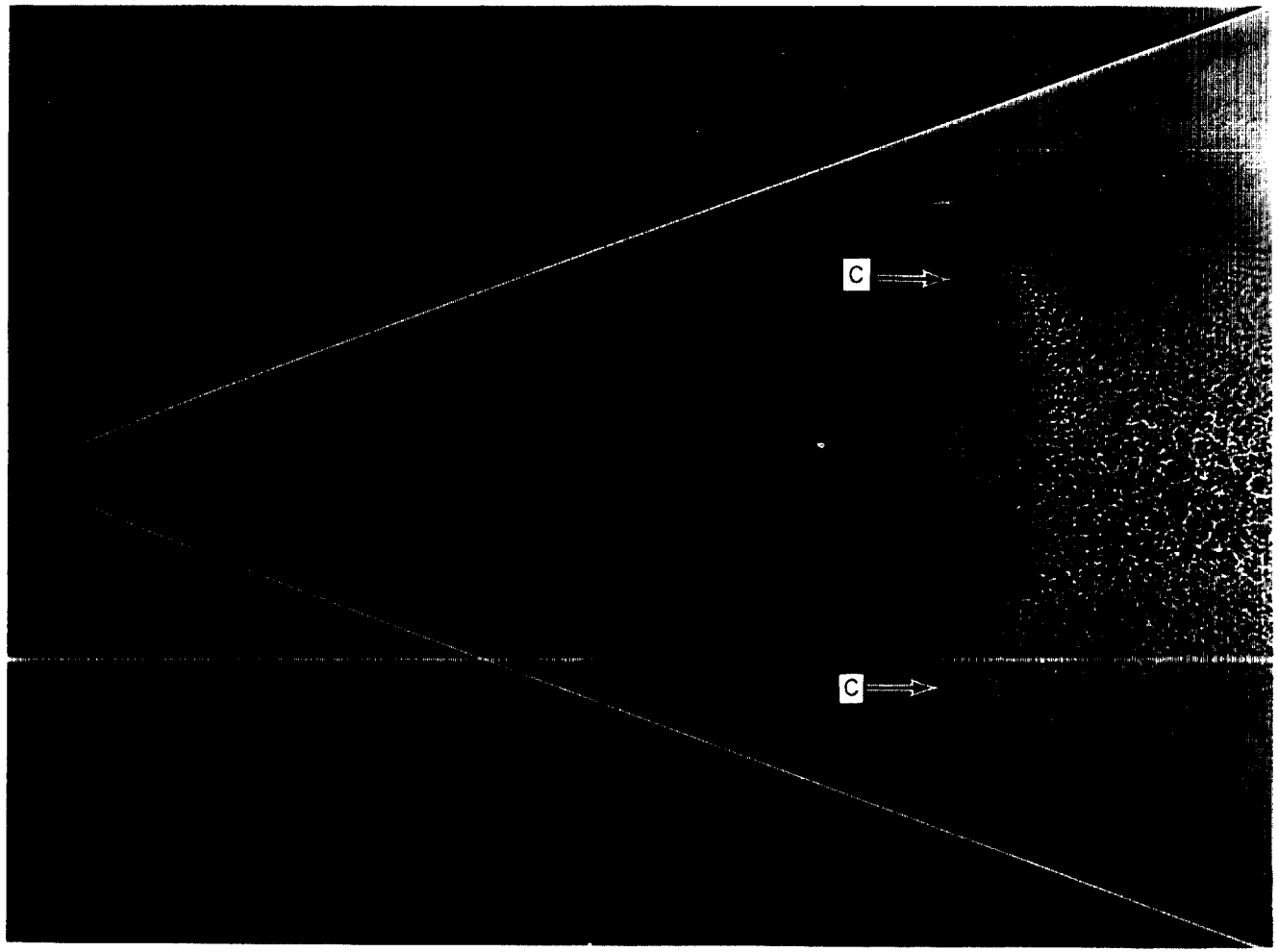

A-27070-C.1

(c) Plan-form view of model 17; $M_\infty = 3.24$.

Figure 6.- Continued.

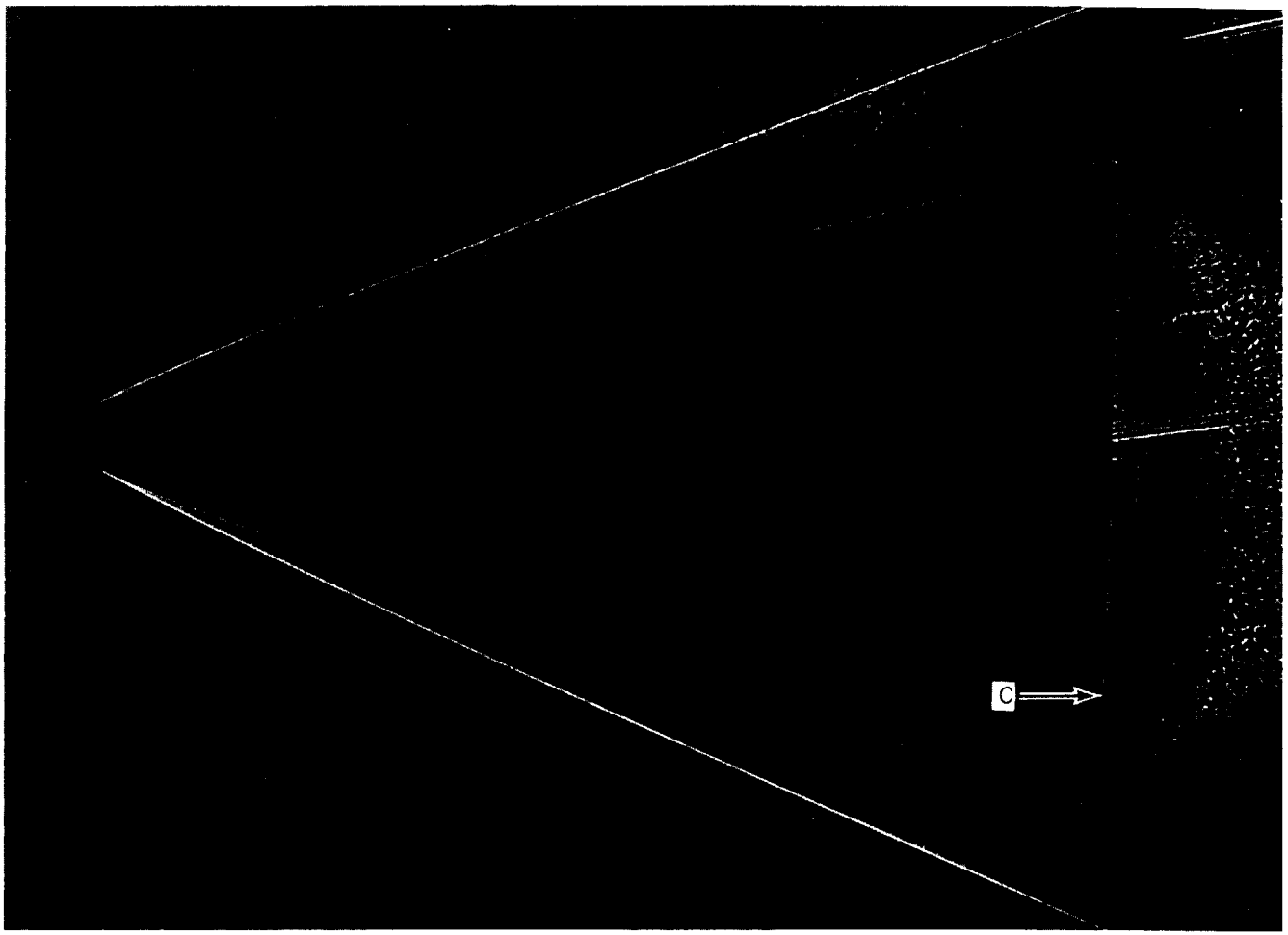

A-27070-D.1

(d) Plan-form view of model 21; $M_\infty = 2.81$.

Figure 6.- Concluded.

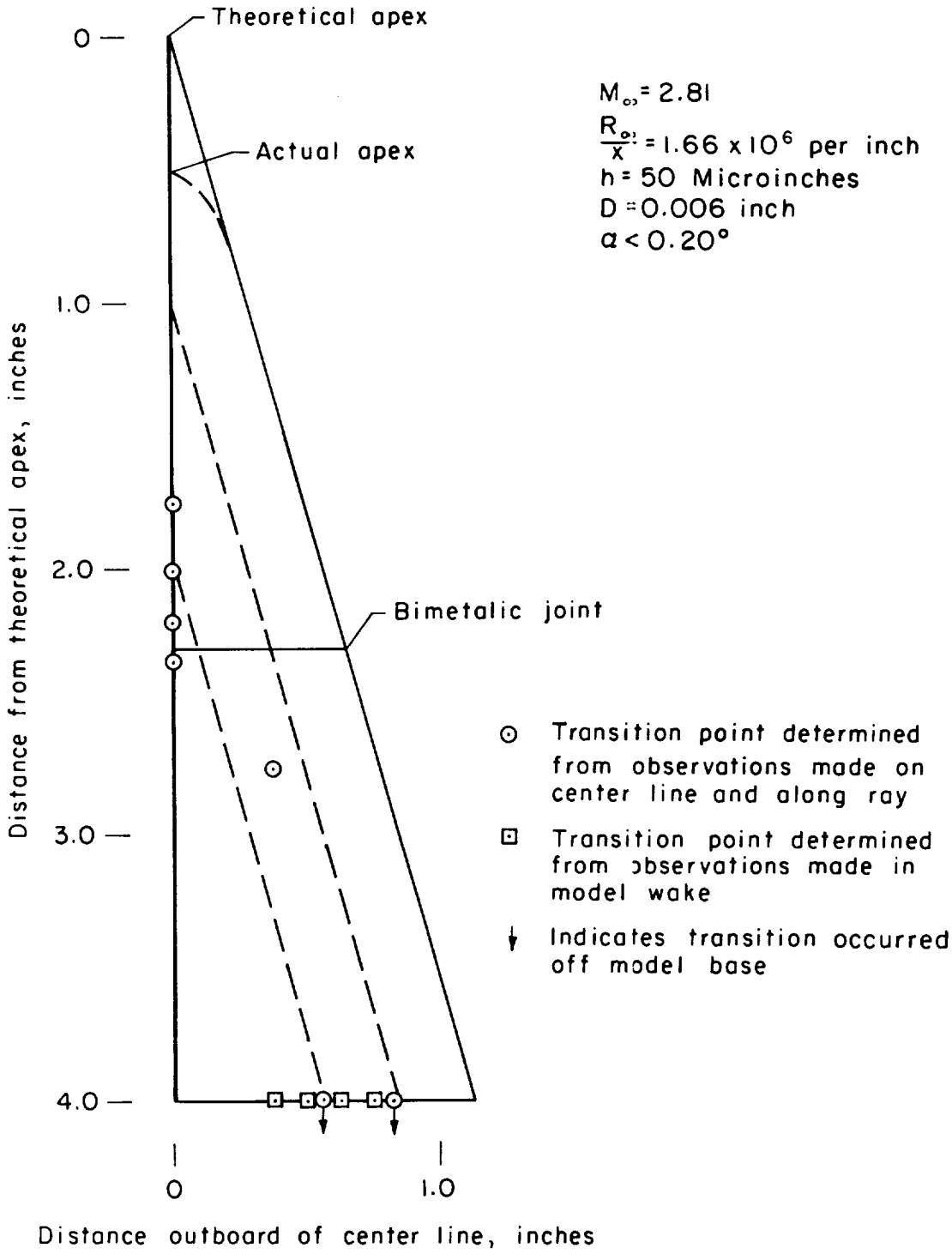

(a) Model 21.

Figure 7.- Plan form of transition pattern.

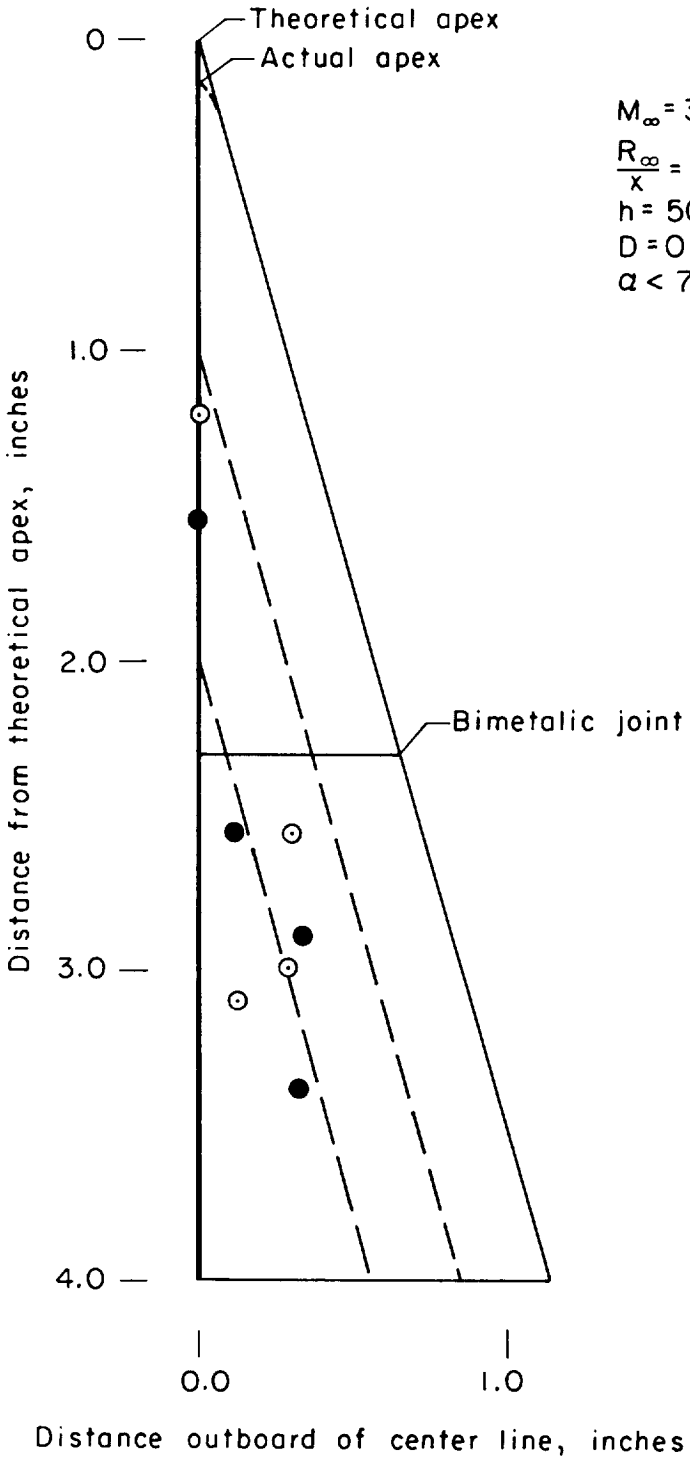

(b) Model 30.

Figure 7.- Continued.

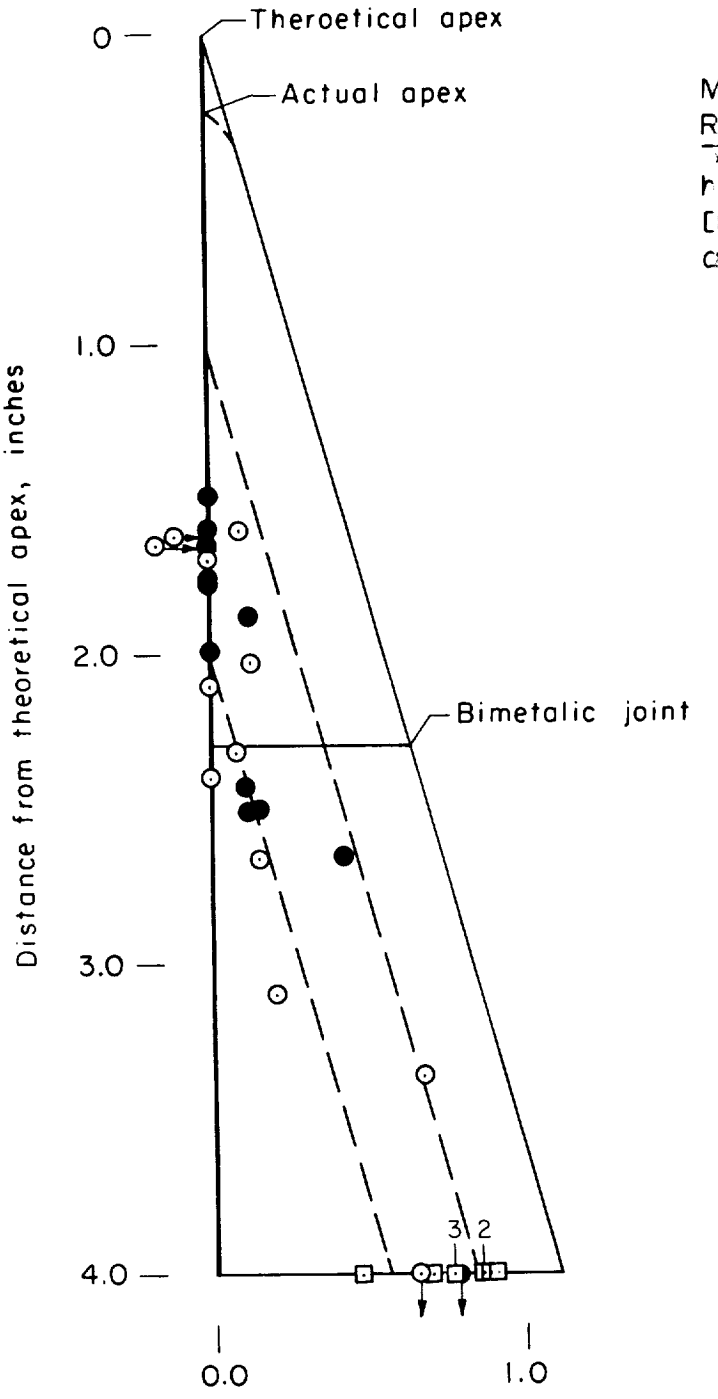

(c) Model 17.

Figure 7.- Continued.

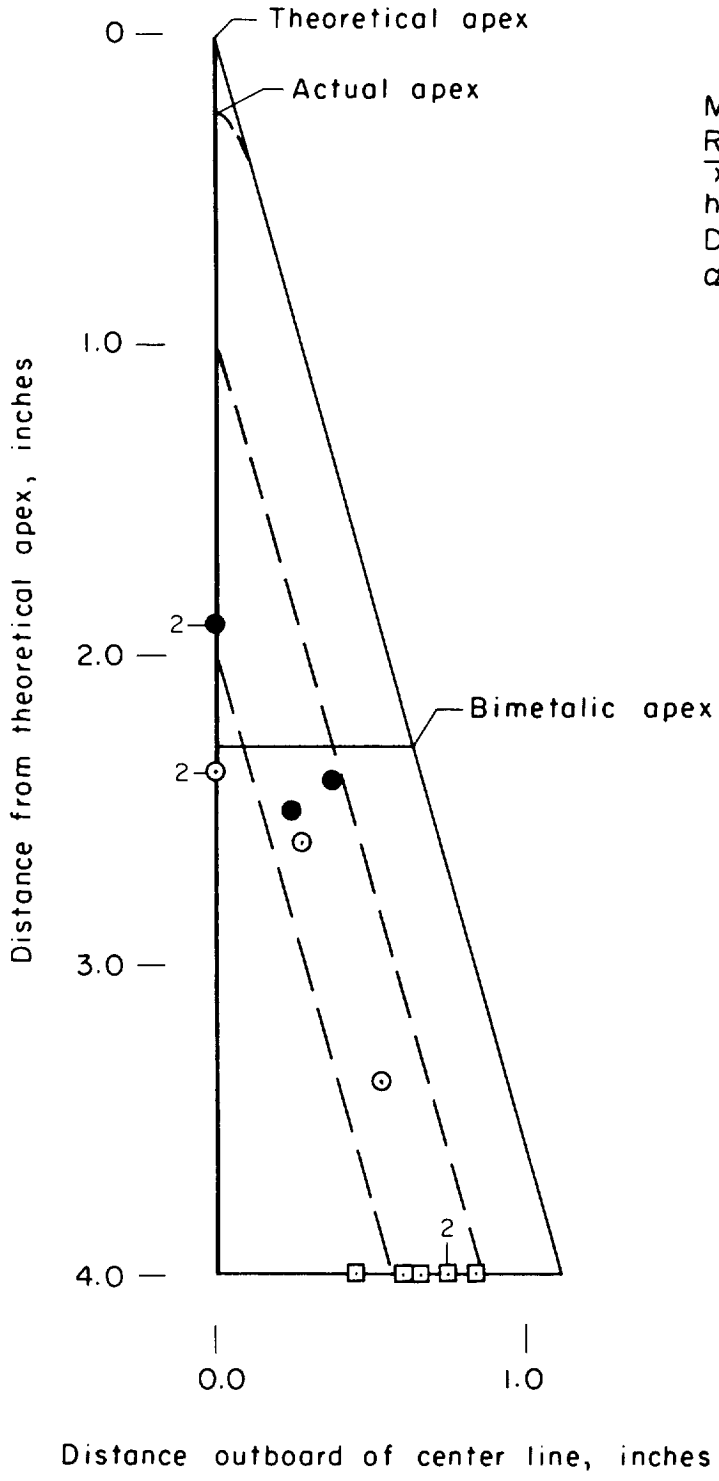

(d) Model 15.

Figure 7.- Continued.

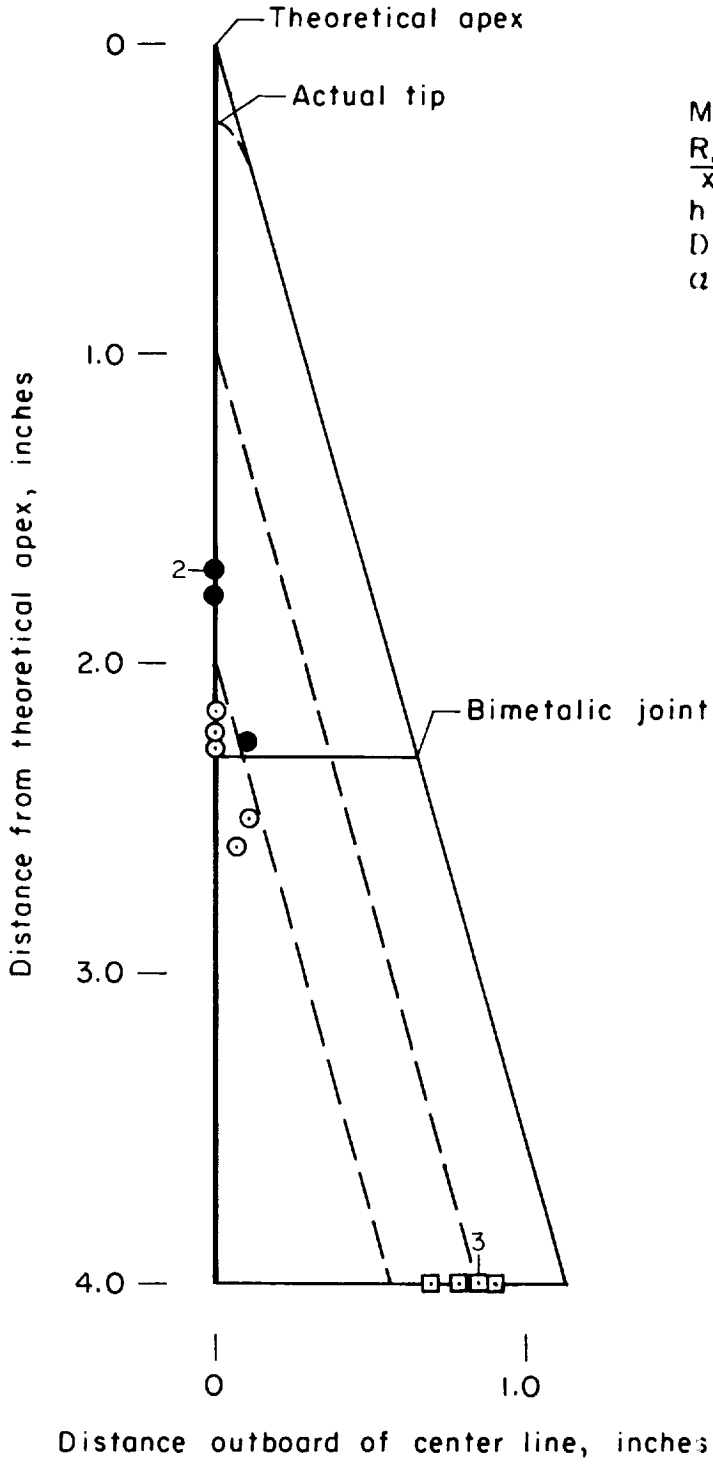

(e) Model 5.

Figure 7.- Continued.

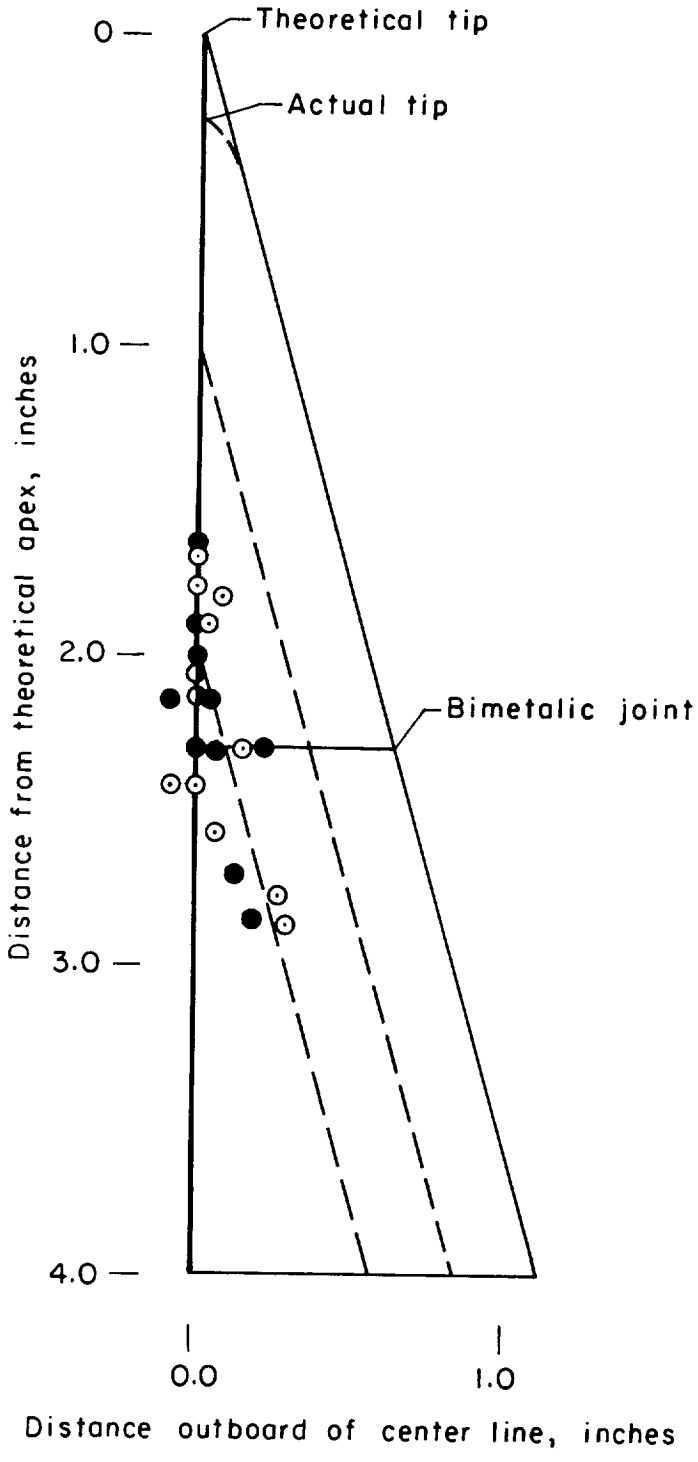

(f) Model 24.

Figure 7.- Continued.

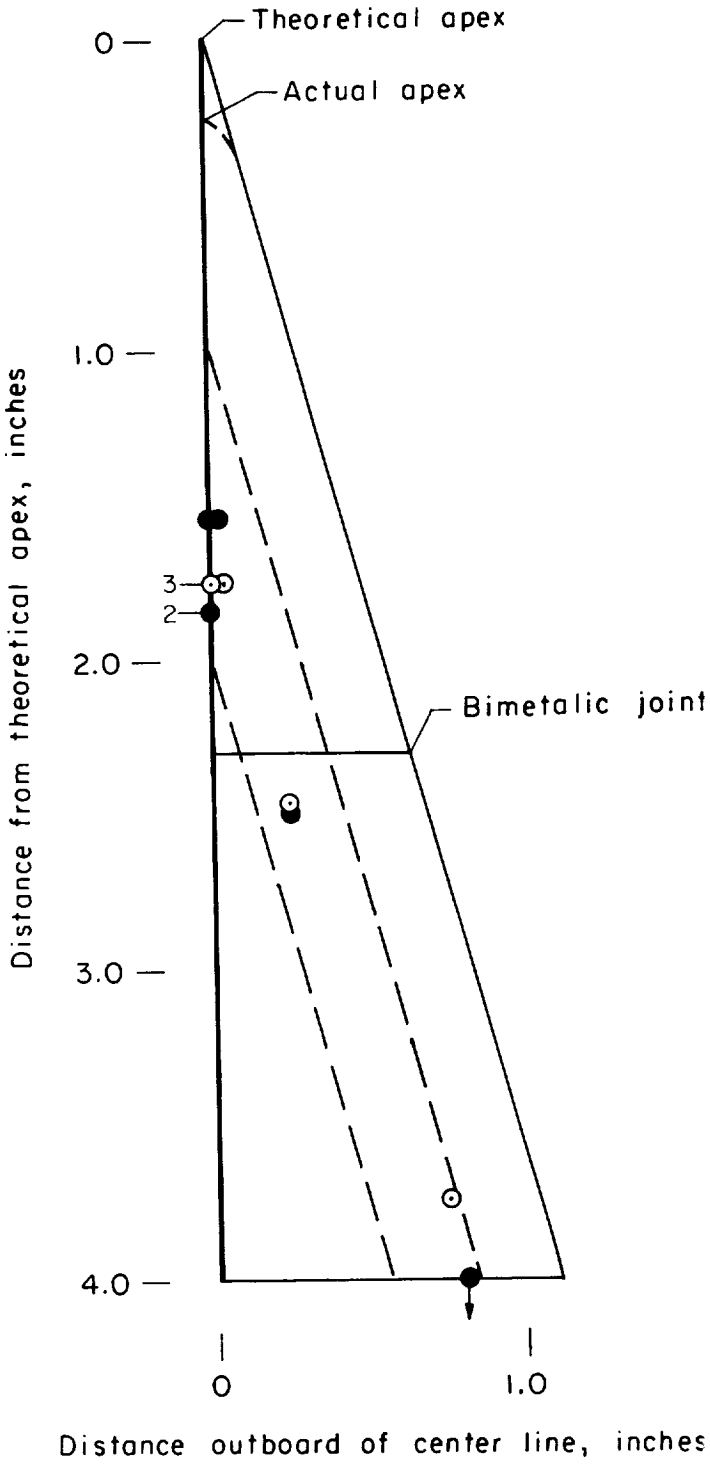

(g) Model 25.

Figure 7.- Concluded.

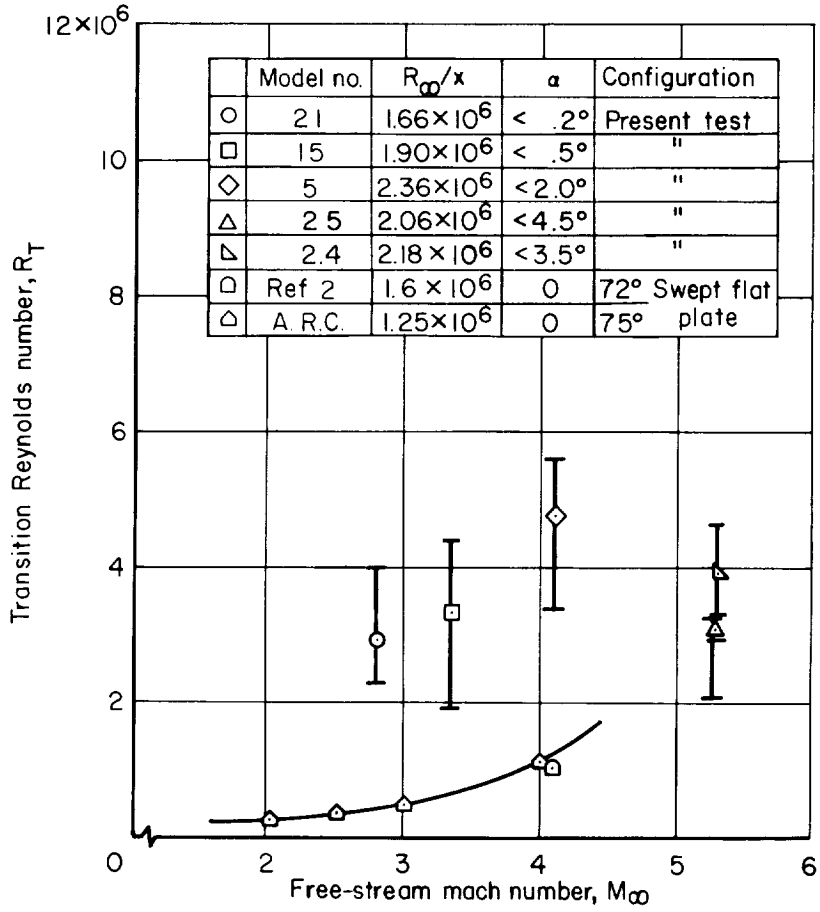

(a) Effect of Mach number.

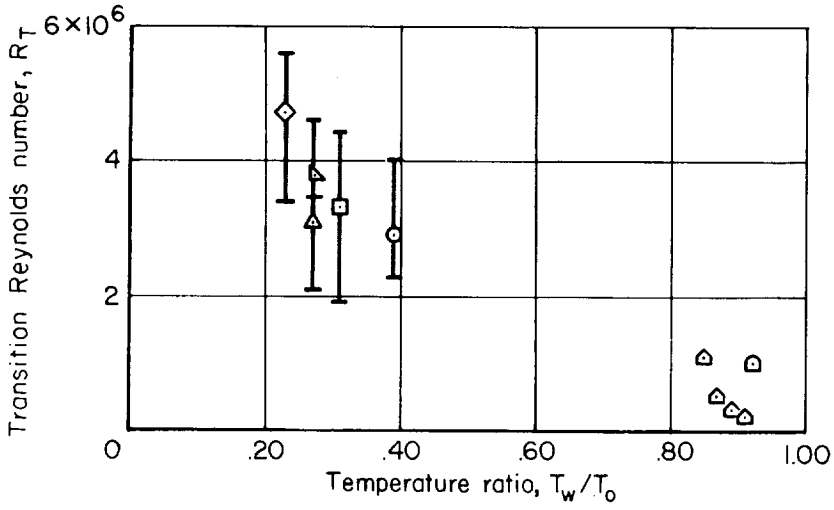

(b) Effect of temperature ratio.

Figure 8.- Effects of Mach number and temperature ratio.

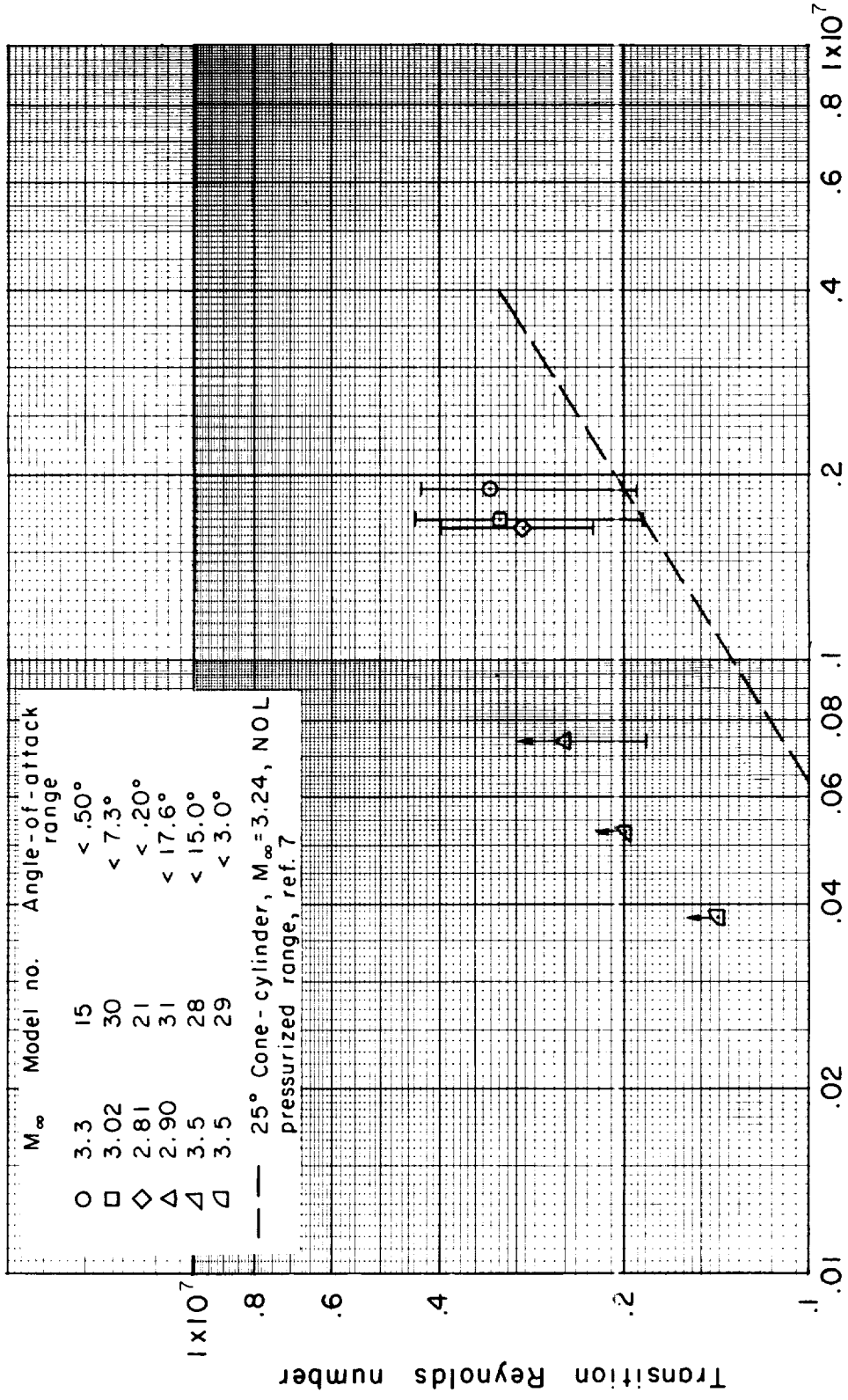

Figure 9.- Effect of unit Reynolds number.

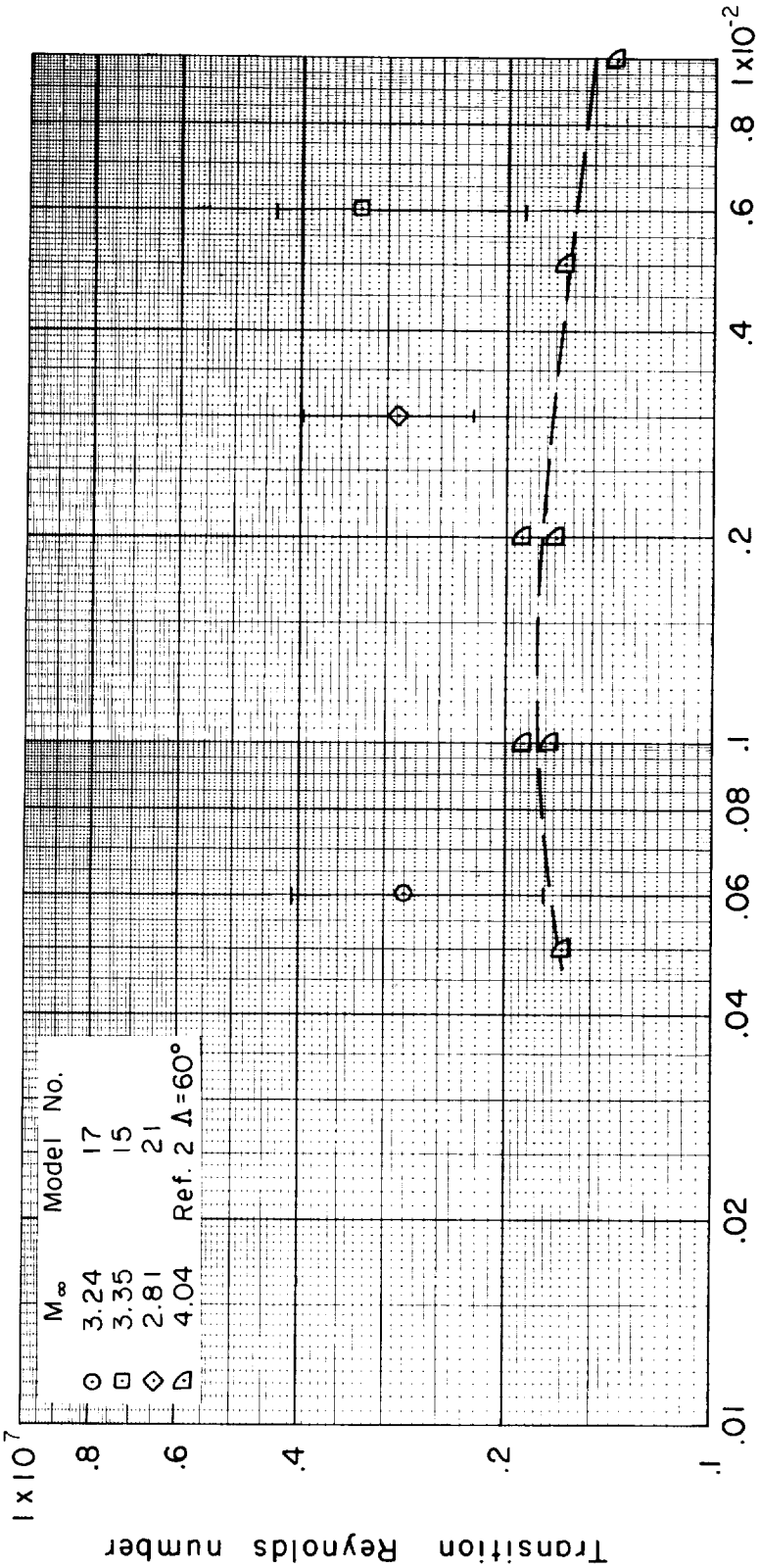

Figure 10.- Effect of leading-edge diameter.

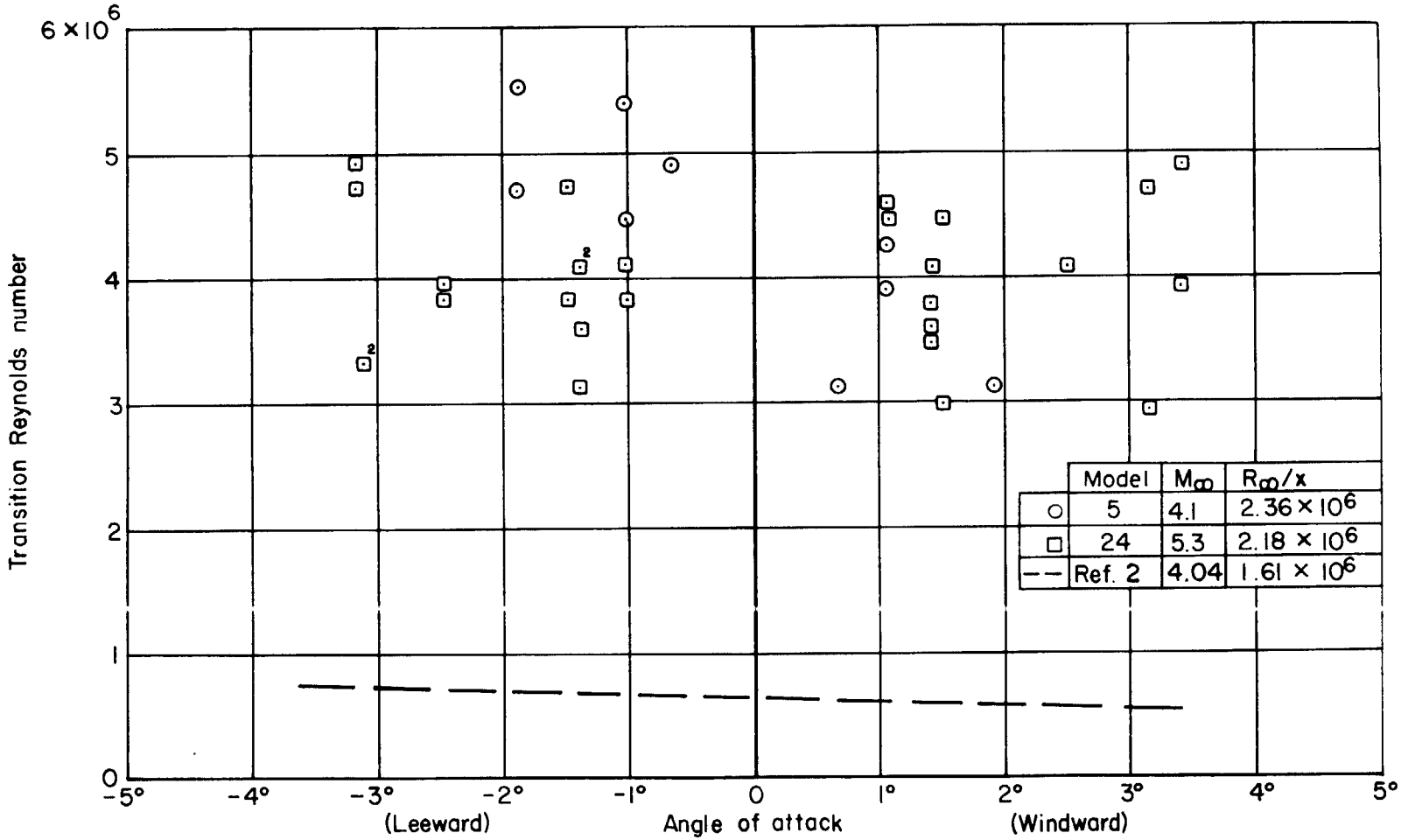

(a) Effect of small angle of attack.

Figure 11.- Effects of angle of attack.

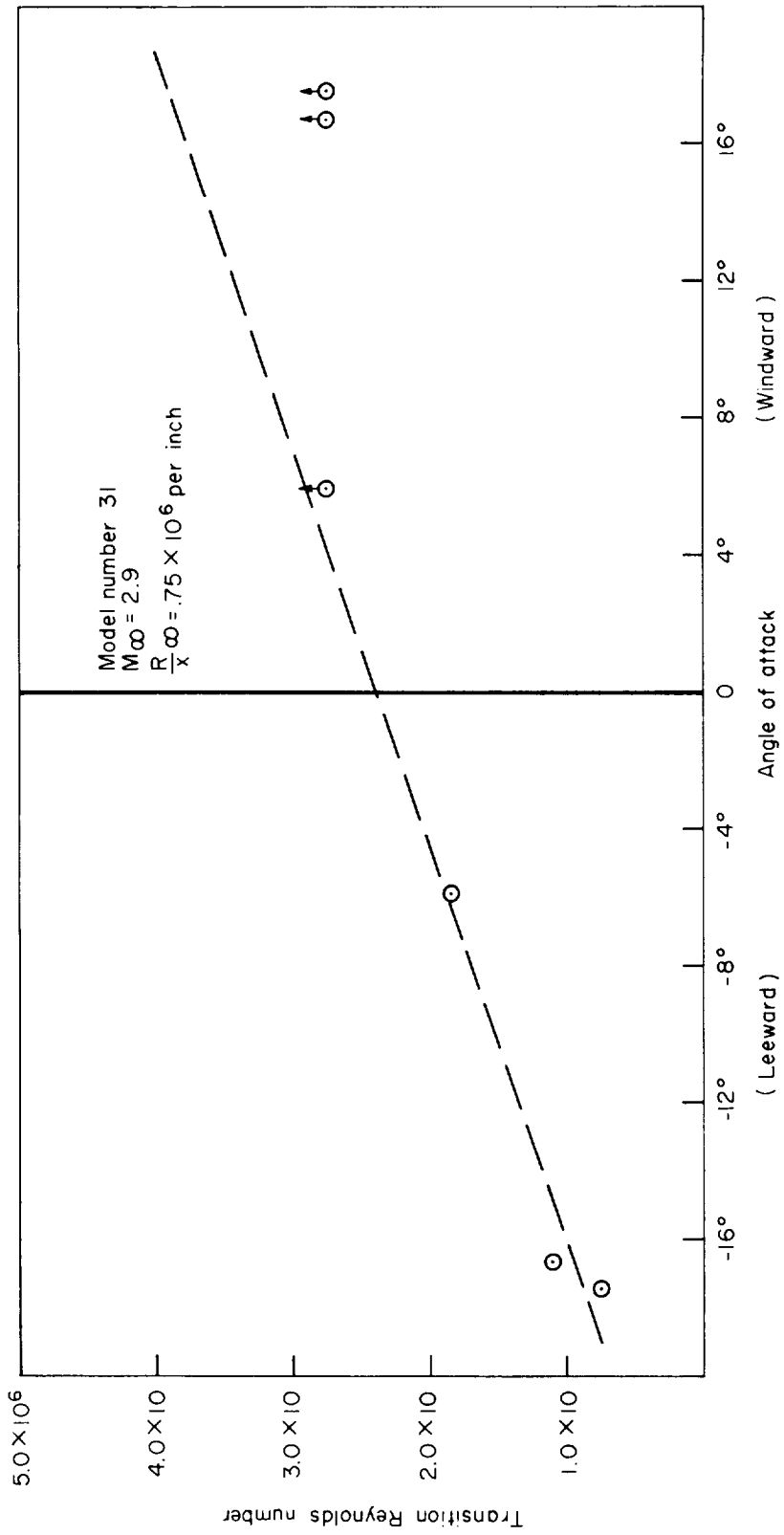

(b) Effect of large angle of attack.

Figure 11.- Concluded.

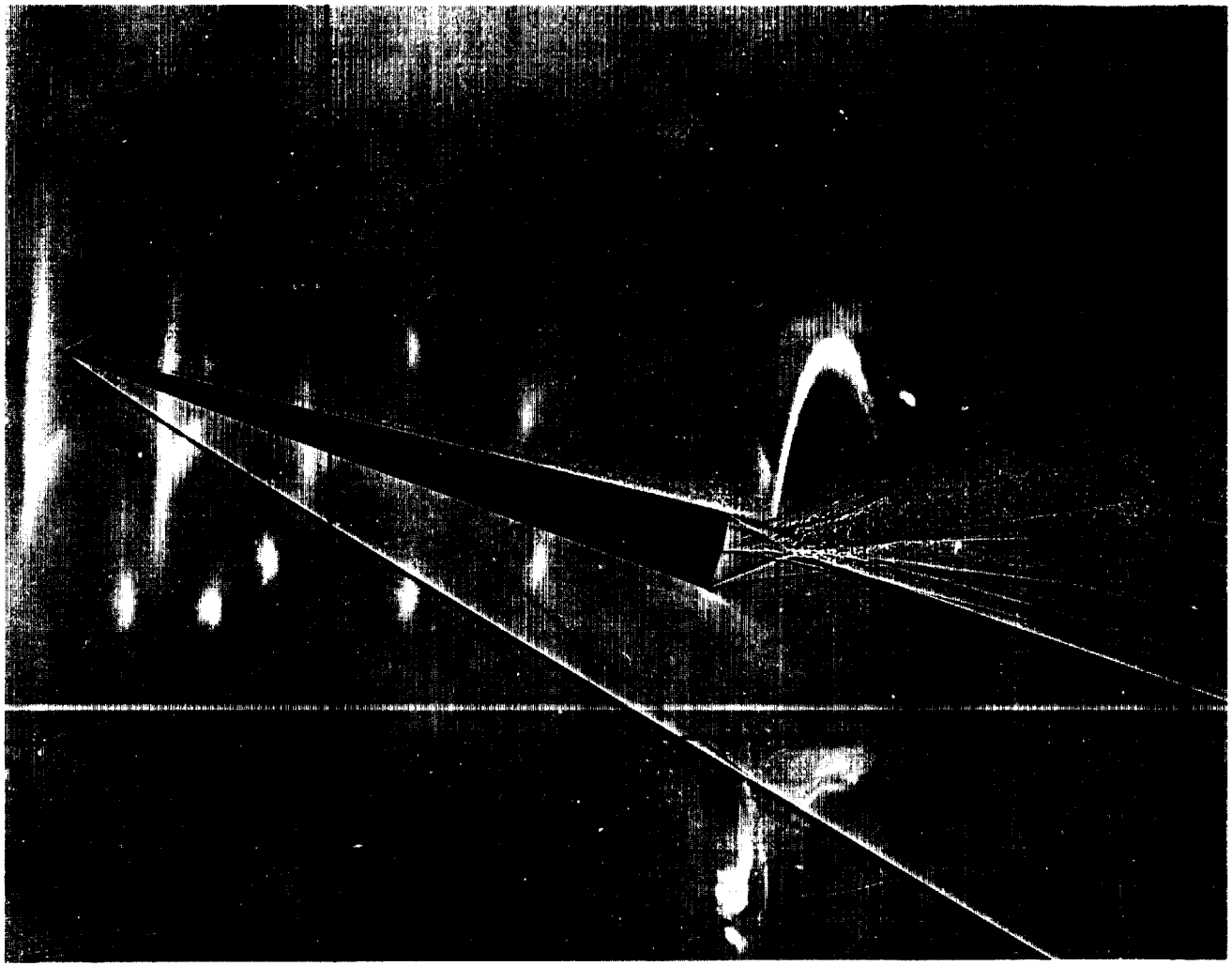

A-27159-B

(a) Model 31; $M_\infty = 2.90$; $\alpha = 16.7^\circ$.

Figure 12.- Delta-wing models in free flight at large angles of attack.

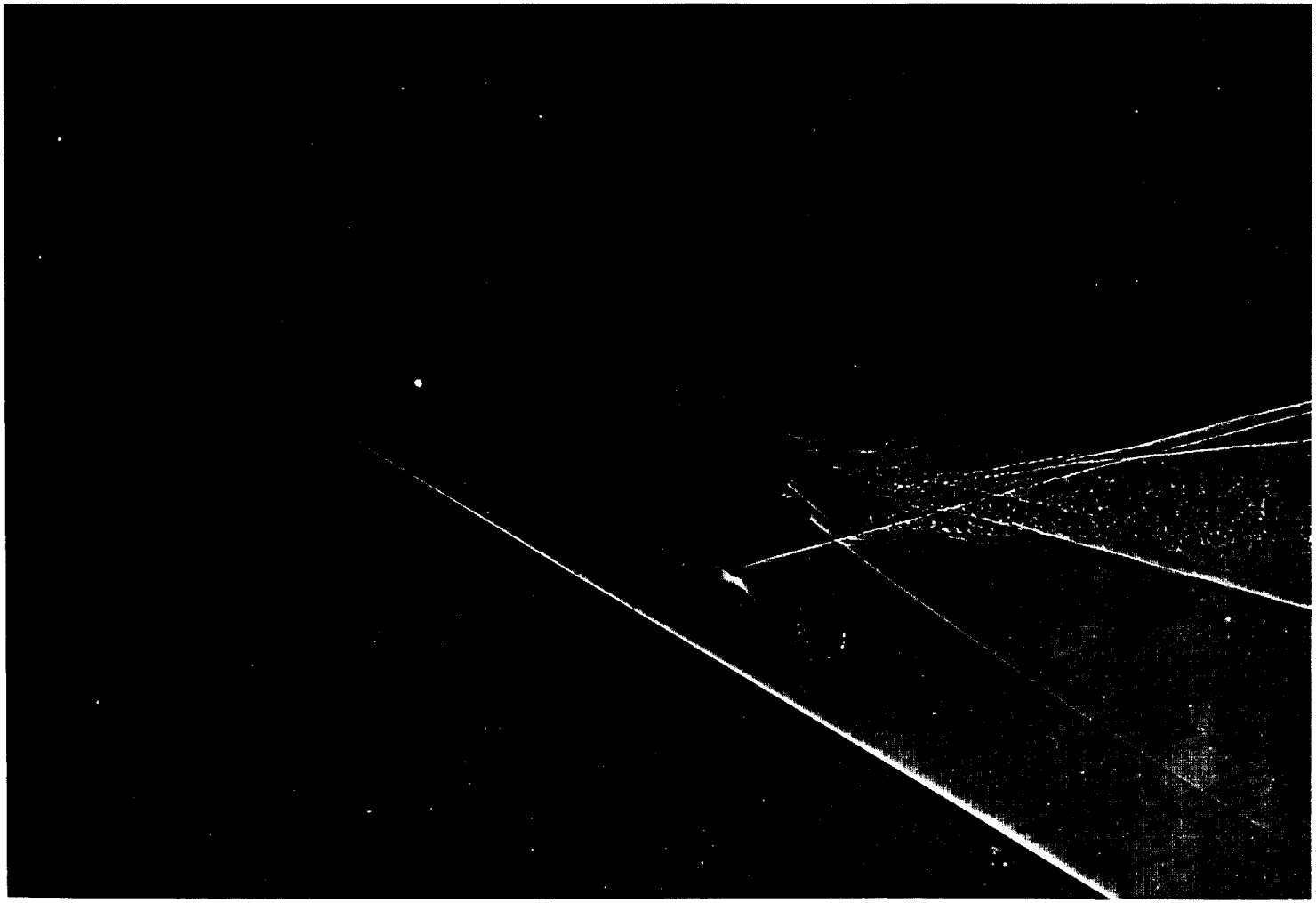

A-27159-A

(b) Model 28; $M_\infty = 3.27$; $\alpha = 25.0^\circ$.

Figure 12.- Concluded.

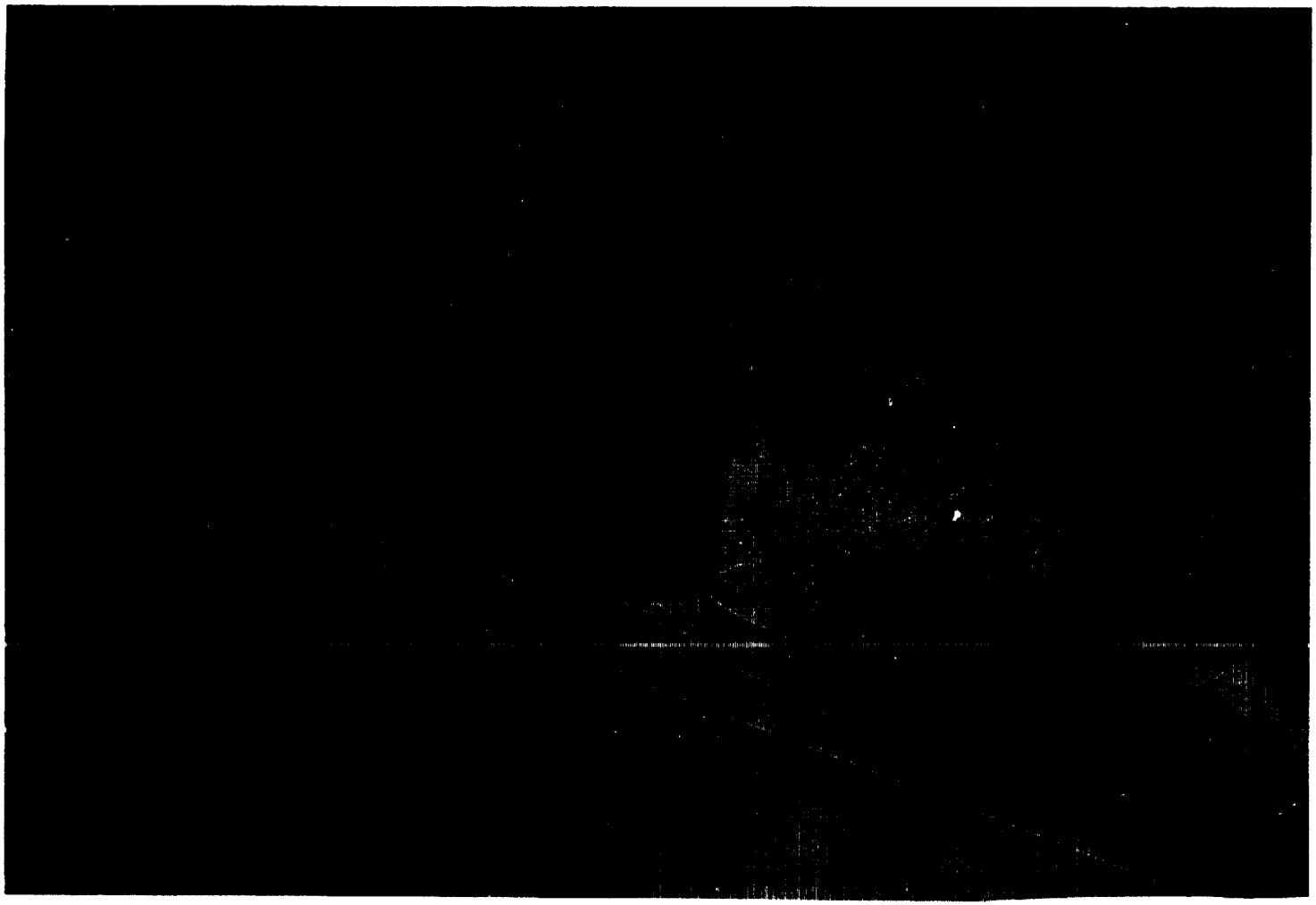

A-27160-C

(a) Model 28; M_∞ = 3.27; R_∞/x = 0.52 million per inch.

Figure 13.- Plan-form views of model wake.

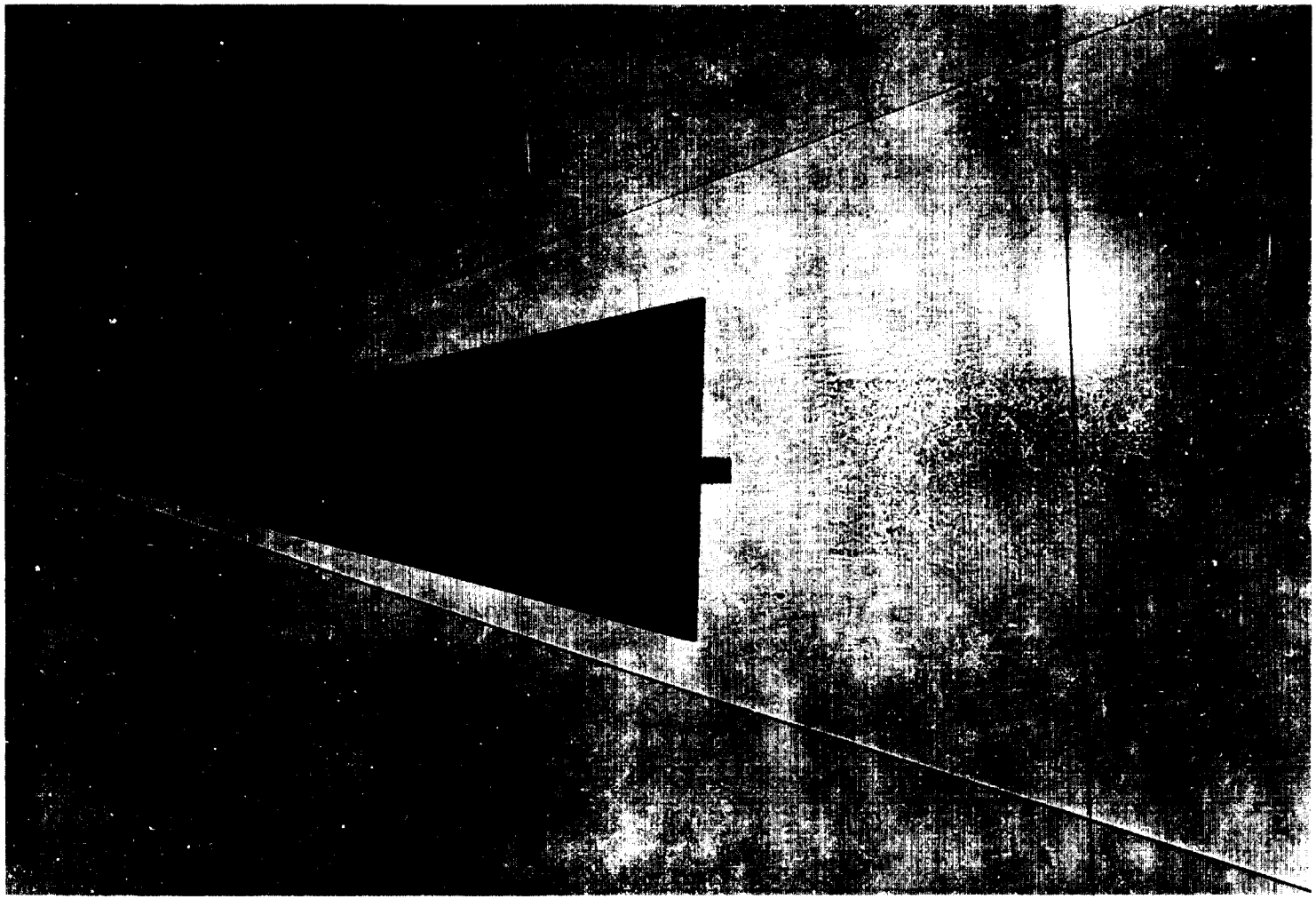

A-27160-A

(b) Model 29; $M_\infty = 3.48$; $R_\infty/x = 0.38$ million per inch.

Figure 13.- Concluded.

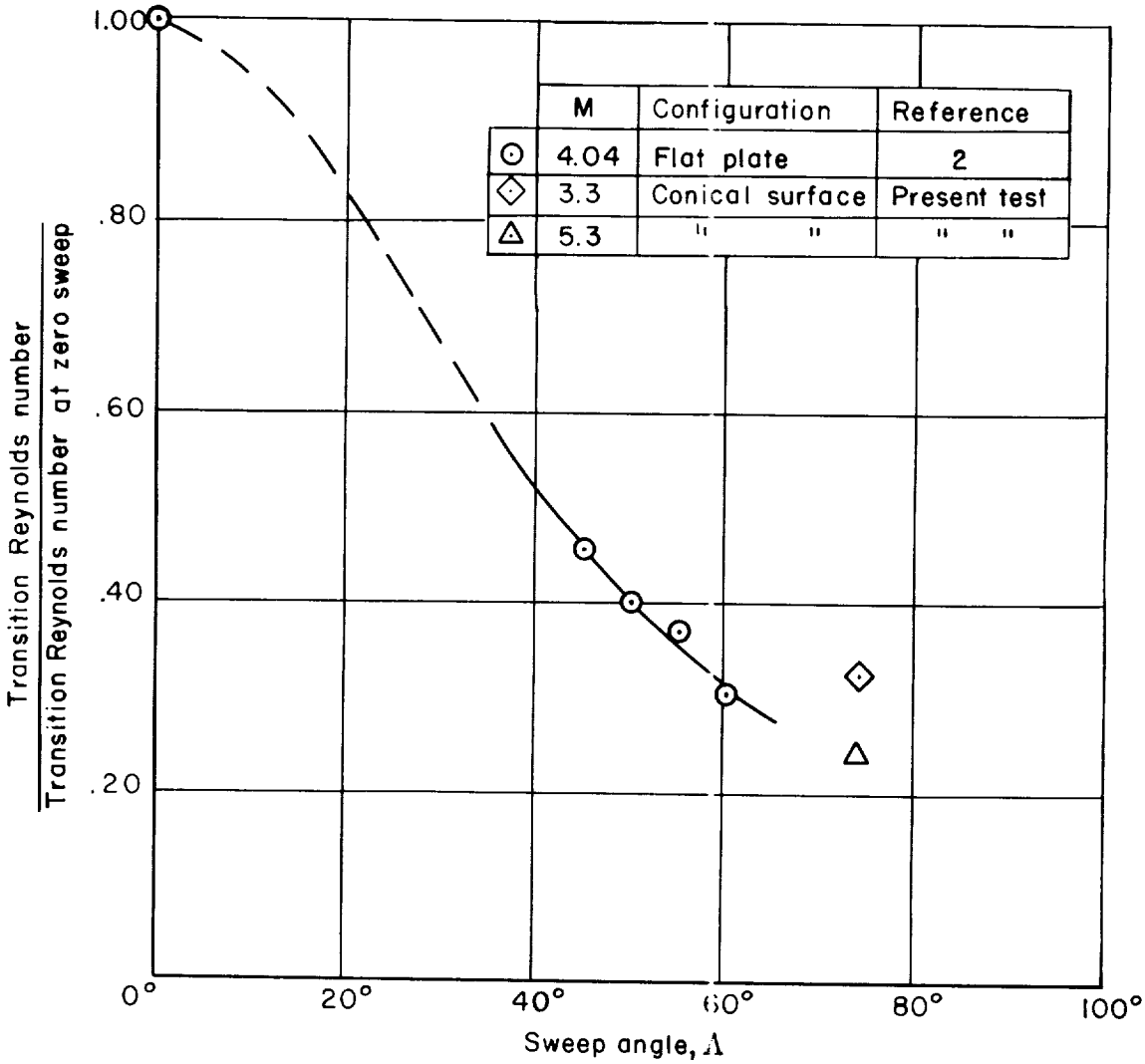

Figure 14.- Effect of sweep on transition Reynolds number.